INVESTIGATION OF ANTITUMOR EFFECTS OF NOVEL ISOXAZOLE DERIVATIVES AND THE ROLE OF BIOTIN CONJUGATION IN THEIR EFFICACY

A THESIS SUBMITTED TO

THE GRADUATE SCHOOL OF ENGINEERING AND SCIENCE

OF BILKENT UNIVERSITY

IN PARTIAL FULFILLMENT OF THE REQUIREMENTS FOR

THE DEGREE OF

MASTER OF SCIENCE

IN

MOLECULAR BIOLOGY AND GENETICS

by

Melike Ergüven

August 2025

INVESTIGATION OF ANTITUMOR EFFECTS OF NOVEL ISOXAZOLE DERIVATIVES AND THE ROLE OF BIOTIN CONJUGATION IN THEIR EFFICACY

By Melike Ergüven

August 2025

We certify that we have read this thesis and that in our opinion it is fully adequate, in scope and quality, as a thesis for the degree of Master of Science.

Onur Çizmecioğlu (Advisor)

Işık Yuluğ

Sreeparna Banerjee

Approved for the Graduate School of Engineering and Science:

Orhan Arıkan
Director of the graduate school

ABSTRACT

INVESTIGATION OF ANTITUMOR EFFECTS OF NOVEL ISOXAZOLE DERIVATIVES AND THE ROLE OF BIOTIN CONJUGATION IN THEIR EFFICACY

Melike Ergüven

M.S. in Molecular Biology and Genetics

Advisor: Asst. Prof. Onur Çizmecioğlu

August 2025

Cancer remains one of the deadliest diseases worldwide. Despite current advancements in the cancer therapeutics, cancer will be global health challenge. Therefore, there is need for development of more effective alternative cancer therapeutics. In this context, here, we evaluated potential of isoxazole-based compounds in cancer therapeutics. In addition to parental isoxazole based-compound EB38, in our study we included biotinylated forms of EB38 (namely compound 160 and compound 161) to assess how biotin conjugation contributes to efficacy of anticancer compounds. To this end, we conducted proliferation assays in 2D cancer models, characterized their pro-apoptotic capacity biochemically, and recapitulated our findings in 3D spheroid models. To investigate the safety of the compounds we used zebrafish larvae to perform toxicity test. We found that EB38 induces anti-proliferative and pro-apoptotic effects in cancer cell lines and more importantly these effects were potentiated with biotin conjugation of compounds. Moreover, we mechanistically identified JAK/STAT pathway as target of EB38 and its biotinylated derivatives.

Additionally, we conducted experiments to understand through which routes biotinylated compounds are accumulated within cells and proposed that alternative, non-competitive mechanism that is not mediated by SMVT might regulate uptake of the biotinylated compounds. These findings suggest that EB38 and its derivatives hold potential for anticancer therapy and that biotin conjugation can serve as a strategy to enhance their therapeutic efficiency.

Keywords: Isoxazole based compounds, biotin-conjugation, JAK/STAT pathway, anticancer therapy, drug uptake, SMVTs

ÖZET

YENİ İZOKSAZOL TÜREVLERİNİN ANTİTÜMÖR ETKİLERİNİN ARAŞTIRILMASI VE BİYOTİN KONJUGASYONUNUN BU ETKİLER ÜZERİNDEKİ ROLÜ

Melike Ergüven

Moleküler Biyoloji ve Genetik, Yüksek Lisans

Tez Danışmanı: Dr. Öğr. Üyesi Onur Çizmecioğlu

Ağustos 2025

Kanser dünya çapında en ölümcül hastalıklardan birisidir. Kanser tedavilerindeki mevcut gelişmelere rağmen kanser küresel bir sağlık sorunu olmaya devam edecektir. Bu nedenle, daha etkili ve alternatif kanser tedavilerinin geliştirilmesine ihtiyaç vardır. Bu bağlamda izoksazol bazlı bileşiklerin kanser tedavisindeki potansiyelini değerlendirdik. İzoksazol bazlı ana bileşik olan EB38'e ek olarak çalışmamızda onun biyotinlenmiş türevleri olan bileşik 160 ve bileşik 161'i de dahil ederek, biyotin konjugasyonunun antikanser bileşiklerin etkinliğine nasıl katkı sağladığı araştırıldı. Bu amaçla, 2 boyutlu kanser modellerinde proliferasyon deneyleri gerçekleştirdik, bileşiklerin pro-apoptotik kapasitelerini biyokimyasal olarak karakterize ettik ve bulgularımızı 3 boyutlu sferoid modellerinde tekrar doğruladık. Bileşiklerin güvenliğini araştırmak için ise zebrabalığı larvaları kullanılarak toksisite testleri yapıldı. EB38'in kanser hücre hatlarında anti-proliferatif ve pro-apoptotik etkiler gösterdiğini ve daha da önemlisi bu etkilerin biyotin

konjugasyonu ile güçlendirildiğini bulduk. Ayrıca, EB38 ve biyotinlenmiş türevlerinin hedeflediği yolak olarak JAK/STAT sinyal yolağını tanımladık. Ek olarak, biyotinlenmiş bileşiklerin hücre içerisine hangi yollarla alındığını anlamak için deneyler yürüttük ve alternatif, SMVT aracılığıyla gerçekleşmeyen ve rekabetçi olmayan bir mekanizmanın biyotinlenmiş bileşiklerin alımını düzenleyebileceğini öne sürdük. Bu bulgular, EB38 ve türevlerinin kanser tedavisinde potansiyeli taşıdığını ve biyotin konjugasyonunun terapötik etkinliği artırmak için bir strateji olarak kullanabileceğini göstermektedir.

Anahtar kelimeler: İzoksazol bazlı bileşikler, biyotin konjugasyonu, JAK/STAT sinyal yolağı, antikanser tedavisi, ilaç alımı, SMVT

ACKNOWLEGEMENTS

First and foremost, I would like to express my heartfelt gratitude to my advisor, Asst. Prof. Onur Çizmecioğlu, for always approaching us with understanding and for being a role model of what it means to be a true scientist. His constant support has been invaluable, and I feel truly privileged to have completed my master's degree under his guidance.

I would like to thank the jury members, Assoc. Prof. Işık Yuluğ and Prof. Dr. Sreeparna Banerjee, for critical reading of my thesis, their contributions, and time.

I am thankful to Prof. Dr. Erden Banoğlu for the synthesis of the compounds that constituted the basis of my work and want to extend my gratitude to Rana Acar, Servin Bagheralmoosavi, and Hazal Beril Çatalak Yılmaz, as well as their research groups, for their valuable contributions to the progress of this project.

I would like to express my gratitude to all members of the OC Lab. From the very first day I joined as a senior student, it has been a great privilege for me to work in such a warm and inspiring environment. I would like to extend my special thanks to Yağmur Öykü Carus, with whom I had the pleasure of working when I first started in the lab. I am deeply thankful to Melda Özge Oğuz for being more of a companion than just a labmate; feeling her constant support has been truly precious to me, and I cannot put into words how grateful I am for her friendship. I would also like to thank Şevval Yılmaz for her motivating words when I was feeling down and for always making me smile. For the great times and conversations, we shared, I would like to sincerely thank Esra Selin Emirmustafaoğlu, Mehmet Gürçay, Özlem Aybüke Işık Bozbey, and Mehmet Burak Taşkaya. The positive and collaborative spirit of our lab is the result of the unique contributions each of you has brought, making this environment truly special and inspiring.

I owe special thanks to my family for always being by my side and supporting me through difficult times and to my dear friends Ayşe Reyyan Kutan, Melike Aydoğan, and Damla Akçaoğlu, Zeynep Akar and Şule Nur Polat. With you by my side, I know I have the greatest friendship in the world.

I also thank TUBITAK for granting me bideb2210A National M.Sc. Scholarship.

DEDICATION

To my beloved Family,

TABLE OF CONTENTS

LIST OF FIGURES

LIST OF TABLES

ABBREVIATIONS

ACC: acetyl-CoA carboxylase

AKT: Protein Kinase B (PKB)

AMP: Adenosine Monophosphate

ASGR: asialoglycoprotein receptor

ATP: Adenosine Triphosphate

BTK: Bruton's Tyrosine Kinase

cGMP: Cyclic Guanosine Monophosphate

PKG: cGMP-dependent kinase

ER: estrogen receptor

FLT3: Fms-like Tyrosine Kinase 3

HDAC: Histone Deacetylase

HCS: Holocarboxylase synthetase

hsp90: Heat Shock Protein 90

JAK Janus Kinase

MCT: Monocarboxylate Transporters

MCC: Methylcrotonyl-CoA carboxylase

NO: Nitric oxide

PDB: Protein Data Bank

PH: Pleckstrin Homology Domain

PI3K: Phosphoinositide 3-Kinase

PIP3: Phosphatidylinositol (3,4,5)-Trisphosphate

PCC: Propionyl-CoA carboxylase

PC: Pyruvate carboxylase

RAF: Rapidly Accelerated Fibrosarcoma Kinase

RAS: Rat Sarcoma Virus Oncogene

sGC: Soluble guanylate cyclase

SMVT: Sodium-dependent Multivitamin Transporter

STAT: Signal Transducer and Activator of Transcription

VEGF: Vascular Endothelial Growth Factor

1. INTRODUCTION

Cancer remains a significant health burden in spite of substantial advancements in the cancer therapeutics. While current developments in the health system -including early diagnosis, surgery, chemotherapy, targeted therapies, radiotherapy- lead to increased survival of patients, there are still serious number of patients dying of cancer (Liu et al., 2024). In 2045, number of people who lost their lives because of cancer is expected to rise to 16.9 million people (all cancer types, both sexes, age [0 – 85+]) while 9.74 million people have died of cancer in 2022 (The International Agency for Research on Cancer (IARC), n.d.). This statistics reveals that cancer continues to be major health concern in the near future. Despite of advanced therapeutic options for cancer, long-term remission of disease is not possible with current treatments due to relapse, toxic side effects, inherent or acquired resistance (Davodabadi et al., 2023). It is imperative that there is need for generation of novel, effective, highly selective towards cancer cells and safer therapeutic alternatives. In this regard, isoxazole-based scaffold containing compounds emerge as promising agents in the field of cancer drug discovery.

1.1. Heterocycles

Increasing urgency for developing novel therapeutic agents for cancer has led to heterocyclic compounds emerging as one of the promising scaffolds and standing out as widely investigated and pharmaceutically relevant scaffolds in the drug discovery (Tandon et al., 2018). Characteristics of heterocycles is to contain at least one heteroatom such as nitrogen, sulfur, oxygen in their ring structures. Heterocycles are frequently preferred in drug developments. Their ability to involve in various molecular interactions such as hydrogen bonding, pi-stacking, metal coordination bonds, van der Waals and hydrophobic forces allows heterocyclic

compounds to engage with binding pocket of target enzyme with in multitude of ways. Moreover, their capacity to appear in diverse ring sizes and structures contributes to their flexibility in use (Tandon et al., 2018). In addition to its structural versality, heterocyclic compounds are widely found in natural compounds such as DNA-RNA bases, vitamins, amino acids. These advantages of heterocycles contribute to their involvement in drug development for cardiovascular, metabolic, and nervous system related diseases as well as cancer and inflammation (Li, 2013). In a study conducted Turanlı et al. (2022), which also constitutes basis of this study, investigated isoxazole- and pyrazole-based compounds, which are subclass of heterocyles, for their in vitro antiproliferative effects and in vivo antitumorigenic capacity. Their findings provided support for potential use of heterocycles in anticancer therapeutics (Turanlı et al., 2022).

1.1.1. Isoxazoles

Isoxazoles are subclass of heterocycles having 5 membered rings with adjacent nitrogen and oxygen atoms. In the drug market, isoxazole rings come in the 33rd place among 351 ring structures, showing their frequent use in the medicinal chemistry (Morita et al., 2018). Presence of electronegative nitrogen and oxygen in the neighboring positions allow isoxazole-based compounds to form hydrogen donor – acceptor interactions with receptors and enzymes, that are not feasible with other ring structures. (Morita et al., 2018)

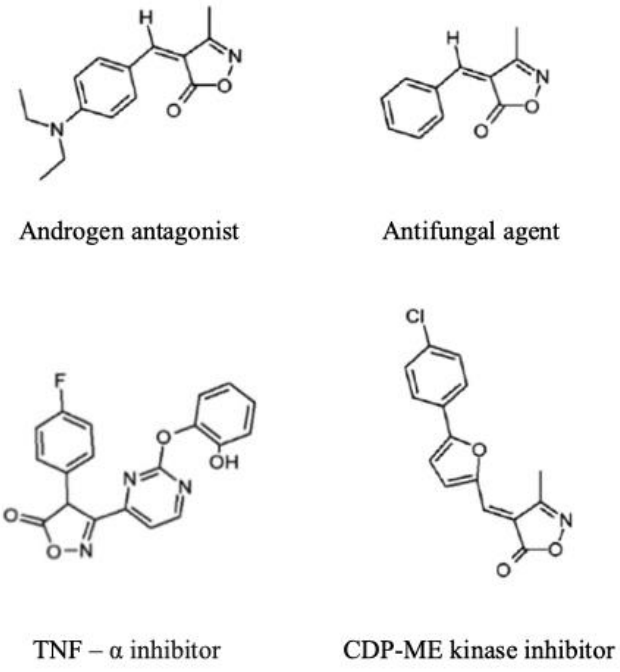

Figure 1. 1. Examples of isoxazole-based compounds with different pharmacological functionalities adapted from Patil et al. (2021). These bioactive compounds have various applications – including cancer therapy, antifungal and antimicrobial activities and immunity-related disease therapy.

Isoxazoles show diverse effects on research settings such as antimicrobial, anticancer, antioxidant, analgesic, anti-inflammatory properties. (Vashisht et al., 2024). These activities of isoxazoles make them promising agents in broad range of therapeutic applications like beta lactam antibiotics (e. g. cloxacillin and dicloxacillin), antibacterials (e. g. sulfisoxazole and sulfamethoxazole), selective COX-II inhibitor (e. g. valdecoxib), immunosuppressive disease-modifying antirheumatic drug (e. g. leflunomide) (Shaik et al., 2020). Examples of isoxazole-ring containing compounds can be found in Figure 1.1.

In addition to well documented bioactivities of isoxazole based compounds in the mentioned areas, they have also attracted considerable attention in cancer research. Considering severe side effects that are posed by current cancer therapeutics, isoxazole based agents appear as promising alternatives due to their milder adverse effects (Arya et al., 2021). So far, recent studies demonstrate that isoxazole based compounds may exert their anticancer properties through activation of cellular mechanisms such as induction of apoptosis, aromatase inhibition, disruption of tubulin congregation, topoisomerase inhibition, HDAC inhibition, ER-alpha inhibition (Arya et al., 2021). These cellular processes are crucial for the survival of cancer cells and the progression of the disease. Targeting these processes with isoxazole-based compounds may have potential to inhibit cancer progression.

Targeting of microtubule is a common strategy employed in current chemotherapeutic agents since it involves in many cellular processes such as motility, maintenance of cell integrity, and division. One of the very recent studies focus on targeting taxane binding site of microtubules with isoxazole based compounds. The most potent isoxazole based compounds appeared to block cells in G2/M phase and disrupt cell integrity pronouncedly without requiring high concentrations of compounds. These findings are promising that current microtubule-targeting chemotherapeutics have significant toxic effects that limit efficiency of treatment. Moreover, they demonstrated that isoxazole-based compounds are effective in exhibiting antitumorigenic properties in docetaxel-resistant prostate cancer, highlighting promising use of isoxazoles to overcome resistance (Peřina et al., 2025).

Furthermore, there are many anticancer agents with isoxazole motifs that are either FDA approved or in clinical trials (Malik & Pal, 2024). HSP90 inhibitor NVP-AUY922 (Luminespib) is in phase II clinical trials (Lee et al., 2011) along with PNZ5 (Montenegro et al., 2016) and XN05 (Wu et al., 2009) which are compounds in clinical trials for gastric cancer and liver cancer patients, respectively. VEGF inhibitor Tivozanib (Sochacka-Ćwikła et al., 2022) and FLT3 inhibitor Quizartinib (Gunawardane et al., 2013) are also classified as isoxazole containing heterocyclic compounds which are FDA approved.

1.2. Biotin and Its Biological Role in Cells

Biotin is known as water-soluble vitamin B derivative and essential for proper functioning of nervous system, development, and growth (Said, 2011). Despite essential requirement of biotin by human cells, it needs to be obtained exogenously from dietary sources through intestinal absorption. There are two routes for biotin supply such as consumption of food that are known to have biotin and microorganisms that are able to synthesize biotin unlike animals. Biotin can minorly be synthesized in humans by microorganisms in the intestines. Therefore, humans primarily meet their need for biotin through food supply (McMahon, 2002).

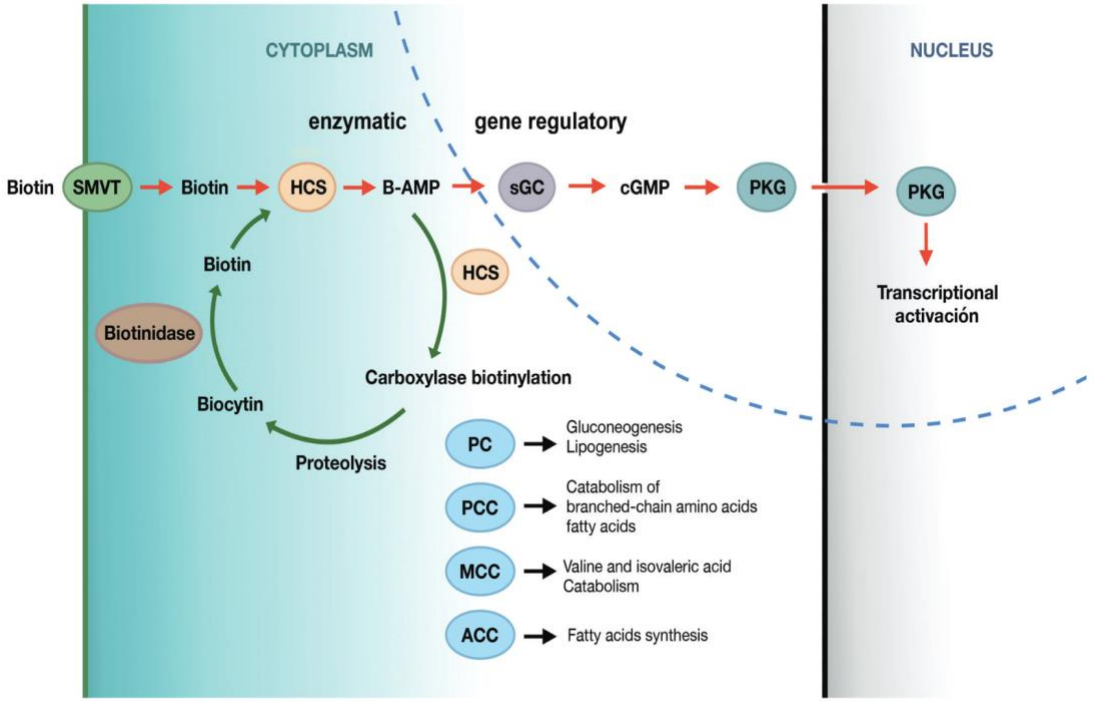

Figure 1. 2. Biotin is taken into cells via SMVT and processed in biotin cycle taken from León-Del-Río (2019). HCS enzyme converts biotin to biotinyl-AMP (active form) and attaches biotin to carboxylases as cofactor. Biotin is proteolytically cleaved by biotinidase to recycle within cell. Biotin regulates gene expression through sGC-PKG axis. Red arrows represent biotin cycle, green arrows represent gene expression regulation.

Biotin is metabolized through biotin cycle in the cells (Figure 1.2) Biotin that is obtained through feeding is usually found to be bound to protein. Protein bound biotins are cleaved by pancreatic enzyme biotinidase. Then, free biotin is taken into cells through canonical SMVTs (sodium dependent multivitamin transporter) on the cellular membrane. Inside of the cell, holocarboxylase synthetase (HCS) enzyme activates biotin in ATP-dependent manner (generating biotinyl-AMP) and catalyzes covalent binding of biotin to carboxylases as cofactors. Inactive carboxylases are named as apocarboxylase. When they are activated upon biotin binding, they are named as

holocarboxylases (León-Del-Río, 2019). Carboxylases regulated by biotin are 1) mitochondrial pyruvate carboxylase (PC) which catalyzes carboxylation of pyruvate into oxaloacetate, which is a key step in gluconeogenesis, lipogenesis, and neurotransmitter synthesis in brain 2) mitochondrial enzyme propionyl-CoA carboxylase (PCC), which catalyzes the carboxylation of propionyl-CoA to malonyl-CoA, which is a key reaction in the breakdown of certain amino acids and fatty acids 3) Methylcrotonyl-CoA carboxylase (MCC) which facilitates carboxylation of 3-methylcrotonyl-CoA to 3-methylglutaconyl-CoA, which is crucial reaction in the breakdown of leucine and isovaleric acid 4) acetyl-CoA carboxylase (ACC) which catalyzes the carboxylation of acetyl-CoA to malonyl-CoA, which is a key step of fatty acid synthesis. (Tong, 2012). To recycle biotin, biotin-bound carboxylases are proteolytically degraded and protein-bound biotin is then subsequently cleaved by biotinidase and it may re-enter into biotin cycle. Overall, participation of biotin as a cofactor of carboxylase enzymes which catalyze essential reactions involved in fatty acid & amino acid metabolism and gluconeogenesis shows its importance in regulation of metabolism (León-Del-Río, 2019).

In addition to its prosthetic role in enzymes, biotin is known to contribute to gene expression regulation and cellular signaling events (Tripathi et al., 2023). Transcriptional levels of certain genes – including glucokinase (an essential enzyme in the glycolysis), phosphoenolpyruvate carboxykinase (an essential enzyme in gluconeogenesis), biotin-dependent carboxylases, holocarboxylase synthetase, SMVTs, cytokines, oncogenes such as n-myc, c-myb, RAS, RAF – are shown to be correlated with biotin levels. These correlations were uncovered upon subjecting cells to biotin deprivation conditions (Rodriguez-Melendez & Zempleni, 2003).

There are proposed mechanisms for the explanation of how biotin contributes to regulation of gene expression. First, biotin acts similar to nitrogen oxide (NO) in cells. It binds and induces conformational changes in sGC (soluble guanylate cyclase) enzyme which increases generation of second messenger cGMP levels in the cells when activated by NO. cGMP-dependent kinase (PKG) is the effector that mediates downstream effects of NO-induced pathway. In hepatocytes, biotin-dependent carboxylases (PC, PCC, ACC-1), primary biotin transporter (SMVT), biotin-attaching enzyme HCS, and ASGR (asialoglycoprotein receptor) are shown to transcriptionally regulated through sGC-PKG axis which is activated by biotin. Specifically, active form of biotin, which is biotinyl-AMP, is shown to activate this axis. Therefore, biotin is mainly said to regulate expression of biotin cycle genes (León-Del-Río, 2019). Another mechanism of regulation of gene expression by biotin is histone biotinylation. Biotinylation of histones (H3 – H4) as post transcriptional modification is a rare biological process catalyzed by enzyme HCS. Biotinylated histones are found enriched in repeat regions and non-transcribed loci in the chromatin. Through modification of histones, biotin participates in genome stability and transcription regulation (Kuroishi et al., 2011).

1.3. Mechanisms of Intestinal Biotin Transport

In humans, biotin is either obtained from dietary sources or synthesized from microorganisms in the large intestines. Then, digested free biotin is absorbed by brush border membrane of enterocytes and biotin synthesized by microorganisms is absorbed in large intestines. Studies performed with vesicles isolated from brush border membrane showed that uptake of biotin into enterocytes is mediated via carriers in Na+ dependent manner. They are able to move biotin against concentration gradient and saturable at micromolar unit. These transportation units are called sodium dependent multivitamin transporters (SMVT). In addition to biotin, they facilitate uptake

of pantothenic acid and lipoate (Said, 2008). However, transportation of biotin across basolateral membrane to release it into bloodstream is not mediated by SMVTs. Expression of human SMVTs is confined to apical membrane (Figure 1.3). Nevertheless, transportation of biotin across basolateral membrane shares a similarity with apical membrane that it is also mediated by carriers but it has Na+ independent mechanisms and electrogenic. Additionally, there is no specifically identified molecule in the basolateral membrane that participates in biotin transportation (Said, 2008).

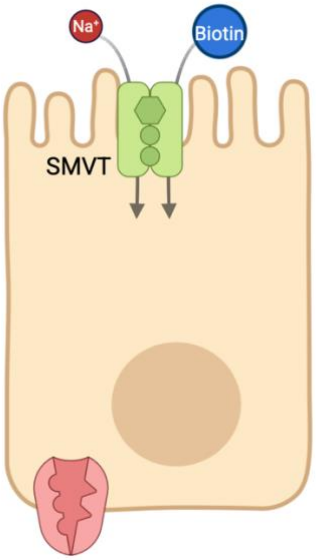

Figure 1. 3. Mechanism of intestinal biotin absorption created with BioRender.com. Biotin is absorbed by SMVT in Na^+ dependent manner by brush border membrane of in enterocytes. Unidentified carrier regulates release of biotin from basolateral membrane of enterocyte.

Mechanisms present in the large intestines to absorb biotin that is synthesized from bacteria is similar to SMVTs on the brush border membrane. Similarly, it acts in Na+ dependent manner and is used by pantothenic acid and lipoate jointly (Said, 1999). Although small intestines are the most

studied organ in the context of SMVTs as it is responsible organ from dietary biotin absorption, SMVT expression is distributed across the body and found in different cells. Placenta, kidney, liver, retina, cornea, cancerous cells are revealed to express SMVTs although they may have varying levels of affinity towards biotin (Vadlapudi et al., 2012). Taken together, SMVTs are considered canonical route for biotin uptake. Nevertheless, alternative mechanisms also contribute to intracellular biotin uptake.

1.3.1. Alternative Routes of Biotin Uptake

MCTs, monocarboxylate transporters, are proposed as alternative mechanisms of biotin transport in lymphoid cells in addition to their ability to express SMVTs (Polyak, 2015). Studies performed with inhibitors and excess competitors of MCT demonstrated reduction in intracellular uptake of biotin in peripheral blood mononuclear cells. It is suggested that MCT works as H^+ dependent anti-transporter for exchange of biotin and monocarboxylic acid like lactate and pyruvate (Daberkow et al., 2003). Also, MCT expression is enriched in many different cancer types from solid tumors to hematological tumors (Singh et al., 2023). It suggests targeting MCT system can also be promising in cancer therapy.

1.4. Biotin Targeted Drug Delivery Systems

Enhancing efficiency of drug delivery to cancer cells is a significant consideration in cancer therapy. In that context biotin conjugation of anticancer agents appears as promising strategy to achieve this goal (Ren et al., 2015). Although SMVTs are regarded as primary route of biotin absorption along with alternative pathways, exact mechanisms underlying how biotin-mediated drug delivery occurs within cells has still been unclear. Despite this ambiguity, significant portion of research which investigate potential targets of biotin-conjugated molecules focuses on SMVTs,

often referring to them as “biotin receptors” although they do not fulfill definition of receptor. (Tripathi et al., 2023). Describing them as “biotin uptake system” is more comprehensive and accurate – given that there are multiple probable mechanisms of biotin uptake exist but are not yet fully identified – but the term “biotin receptors” is widely used in the literature.

There are multiple studies revealing that cancer cells overexpress biotin receptors in comparison to healthy cells. Overexpression of biotin receptors in cancer cells makes them important target of cancer therapeutics while sparing healthy cells from toxic effects of anticancer agents and increasing efficiency of parental anticancer agents. The pioneering study demonstrating the overexpression of biotin receptor in cancer cells is conducted by Russell-Jones et al. (2004) where uptake of polymers conjugated with either biotin, B_{12}, or folate (and non-conjugated) were investigated. Comparative study performed on over 15 cancer cell lines revealed that cancer cells either showed enhanced uptake of folate or B12 conjugated polymers or didn’t exert selective advantage toward any polymer. More importantly, cancer cells that overexpress folate or B12 receptors also overexpress biotin receptor and among these three conjugations, biotin conjugated polymers are found to be most significantly taken inside of cancer cells. In vivo experiments also demonstrated that among different conjugations, doxorubicin-polymer targeted with biotin resulted in the greatest tumor reduction although reduction of tumor weight is less than anticipated (Russell-Jones et al., 2004).

After that study, targeting of cancer cells with biotin conjugation grabbed significant attention in the field of cancer therapeutics. In a study conducted by Jung et al. (2014) revealed that biotin conjugated coumarin (fluorescence signal) exhibited increased fluorescence signal in A549 cancerous lung cells compared to WI38 normal lung cells. This study shows that biotin conjugated

molecules can be used as cancer-specific probe (Jung et al., 2014). Another study conducted by the same research group also revealed that biotin conjugated gemcitabine, a chemotherapeutic agent, reduced viability to approximately 20% while 70% of only gemcitabine treated A549 cells survive (Maiti et al., 2013). These two studies show that biotin conjugated molecules can selectively act on cancer cells and more efficiently compared to parental molecule.

Contrary to the common presumption that biotin mediated drug delivery occurs predominantly through SMVTs, there are many issues that need to be resolved about SMVTs. First, biotin conjugated molecules are usually synthesized through amidation or esterification of carboxylic acid, which is critically important for recognition of biotin by SMVTs. Interestingly, loss of free carboxyl group during conjugation didn't impair biotin-mediated delivery (Tripathi et al., 2023). Second, SMVTs are known to transport small molecules like biotin, pantothenic acids etc. However, there are studies focusing on biotin-mediated delivery of large molecules such as polymers, polypeptides (Tripathi et al., 2023). Third, biotin transporters generally have K_m value in micromolar range while nanomolar range of biotin-conjugated molecules are shown to be still effective in studies (Tripathi et al., 2023). These questions may suggest that this process is not exclusively SMVT-mediated, suggesting the involvement of other biotin uptake mechanisms.

For instance, Pandeya et al. (2021) demonstrated that fluorescent probe, Atto565, is efficiently accumulated in the gram-negative bacterial cells. However, competition with free biotin didn't lead to impaired intracellular accumulation of fluorescent probe, suggesting SMVT- independent non-competitive uptake of biotin (Pandeya et al., 2021). Along the same lines, Subedi et al. (2020) showed that attachment of cancer cell lines (Hela and MCF7) to biotinylated surfaces was

improved in the presence of free biotin, but not by folic acid (Subedi et al., 2020). These studies suggest alternative mechanisms of biotin uptake.

1.4.1. Advantages and Challenges of Biotin Mediated Drug Delivery

Recently, chemotherapeutic agents which induce systemic side effects on patients are combined with targeted agents to lessen side effects. By doing so, intracellular uptake of agents is aimed to increase while minimizing side effects which may lead to abandonment of treatment regime. In that context, biotin conjugation of anticancer agents appears as promising approach since biotin conjugation of anticancer agents allows selective uptake by cancer cells while sparing normal cells due to significant overexpression of biotin receptors in cancer cells (Wang et al., 2024). Since cancer cells are able to internalize biotin conjugated agents more efficiently compared to normal cells, more effective antitumor responses can be obtained more easily without needing to elevate concentration of anticancer agents, contributing to minimized side effects on healthy cells. Ovarian, breast, and lung cancer are known to be effectively responsive to biotin-mediated drug delivery. Additionally, biotin receptors are presented as more specific target compared to other vitamin receptors such as folate receptors. By doing so, more precise delivery of anticancer agents can be achieved, lowering adverse side effects. Also, ability of biotin to be attached to various molecules such as chemotherapy agents, protein-based drugs, and genes broaden its applicability and flexibility (Wang et al., 2024).

Significantly, it is shown in Lv et al. (2016) that biotin-decorated nanocarriers encapsulating chemotherapeutic doxorubicin and chemo-sensitizer quercetin exhibited increased cytotoxicity and reduced drug efflux in doxorubicin resistant MCF7 cells and improved drug accumulation and

antitumorigenic effect in vivo compared to non-biotinylated nanocarriers (Lv et al., 2016). This result may suggest potential use of biotin conjugation to reverse multidrug resistance in breast cancer. Ability of biotin decorated nanocarriers to deliver two drugs simultaneously help to resolve problem of resistance, a significant issue in therapeutics.

Contrary to advantages of biotin-mediated drug delivery, it possesses multiple challenges in clinics. Overexpression of biotin receptors exhibits broad cell specificity, not all cell types express biotin receptor to the same extent. For example, MDA-MB-231 and MCF-7 cell lines are known to overexpress biotin receptors while MDA-MB-157 cells expresses biotin receptor to a lesser extent. This highlights the importance of molecular subtypes of tumors while designing biotin-mediated delivery (Wang et al., 2024). From a clinical translation perspective, it is anticipated that therapeutic benefit of biotin conjugation may be limited to selected patient populations, emphasizing the importance of personalized medicine.

SMVTs, which are regarded as primary mechanism of biotin mediated delivery, acts in a sodium-dependent way, whose activity is inhibited by exchange of sodium with other molecules like choline, lithium, or ammonium. Therefore, sodium is required in the tumor microenvironment to obtain efficient delivery of biotin conjugated drugs into tumor cells. Therefore, it is essential to test efficacy of biotin-mediated delivery in physiological environment (Wang et al., 2024). Also, it should be noted that level of endogenous biotin may interfere with efficient uptake of biotinylated agent, competing with the drug itself. Moreover, attachment of biotin to drugs may affect permeability of drugs due to enlarged size of new drugs, affecting efficiency of drug delivery (Wang et al., 2024).

1.5. Rationale and Aim of the Study

In this study, we built upon previous research where novel vicinal diaryl substituted isoxazole (EB38) were demonstrated to have antitumorigenic capacity. Given its potent antitumorigenic properties – including inhibition of tumor growth in breast and liver xenografts and induction of apoptosis – we desired to further enhance its efficiency by utilizing biotin-conjugated derivatives of EB38, namely biotinylated compound 160 (C160) and PEG-biotinylated compound 161 (C161). As mentioned in the introduction section, biotin-conjugation of compounds can be exploited to improve efficiency anticancer therapy. Our aim was to assess impact of biotin conjugation of isoxazoles on their antitumorigenic efficacy. Furthermore, we desired to understand molecular targets of EB38 and its biotinylated derivatives to identify signaling pathways involved in anticancer activity of EB38 and its derivatives. This work can provide better understanding for development of more effective anticancer compounds.

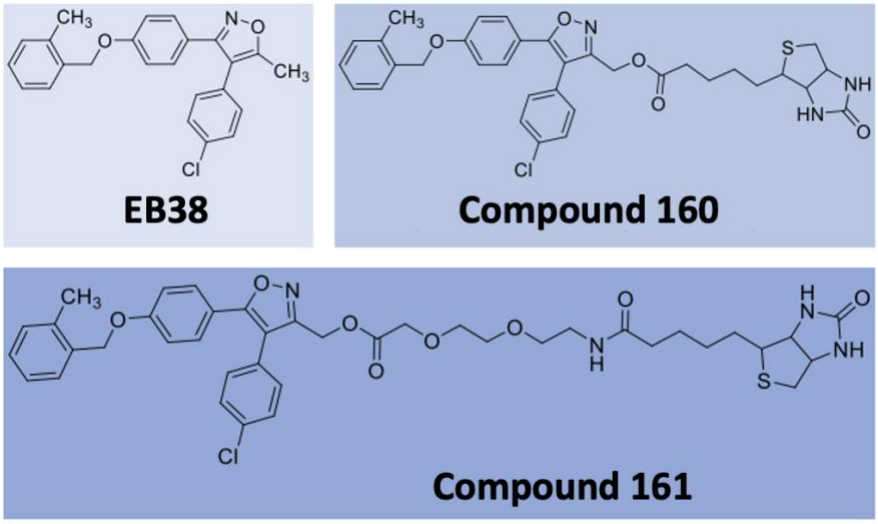

Figure 1. 4. SMILES notation of EB38, Compound 160, and Compound 161. EB38 is the parental isoxazole based compound. C160 is the biotin conjugated derivative of EB38 while C161 is PEG-biotin conjugated derivative of EB38.

2. MATERIALS & METHODS

2.1. MATERIALS

2.1.1. Materials Used in Cell Culture

CATALOG NUMBER	PRODUCT NAME	BRAND NAME
Gibco	High Glucose DMEM	41966-029
Gibco	RPMI – 1640	21875-034
Gibco	DMEM/F12	11320-074
Capricorn Scientific	Fetal Bovine Serum	FBS-16A
Capricorn Scientific	Penicillin – Streptomycin	PS-B
Diagnovum	Insulin	D630
GenScript	Epidermal Growth Factor (EGF)	Z00333-1
Sigma-Aldrich	Non-Essential Amino acids	M7145
VivaCell	L-glutamine	C3543-0100
Sigma-Aldrich	Hydrocortisone	H0888
Biowest	Trypsin (0.5%)	X0930
Gibco	Trypsin (0.25%)	25200-056
Serva	DMSO	20385.02
MedChemExpress	GDC-0941	HY-50094
Gibco	Puromycin	A11138-03
Thermo Fisher	Mr. Frosty™ Freezing Container	5100-0001

2.1.2. Materials Used in Proliferation Assay

CATALOG NUMBER	PRODUCT NAME	BRAND NAME
Sigma-Aldrich	Sulforhodamine B	S9012
Merck	Trichloroacetic Acid	27242
Isolab	Acetic acid	901.013
Sigma Aldrich	Tris-base	T1503

2.1.3. Materials Used in Western Blotting

CATALOG NUMBER	PRODUCT NAME	BRAND NAME
Intron Biotechnology	RIPA	IBS-BR002a
Sigma	Sodium orthovanadate	S6508
GlpBio	Protease Inhibitor Cocktail	GK10014
Serva	Phosphatase Inhibitor Mix II	39055.01
Carlo Erba	Ammonium Persulfate	410627
Serva	TEMED	35925,01
Serva	Acrylamide/Bis Solution	10688.01
TaKaRa	BCA Protein Assay Kit	T9300A
Ecotech	Laemli Sample Buffer	LSB-4X
Applichem	Beta mercaptoethanol	A1108.0100
neoFroxx	Glycine	1154KG001
Merck	SDS	822050.1000
Applied Biological Materials	Protein Marker	G623

GVS	Nitrocellulose Membrane	1212632
Ecotech	Ponceau S	PS05
Capricorn	Bovine Serum Albumine	BSA-DG
Serva	Sodium Azide	30175.01
Serva	Tween-20	39796.01
Advansta Inc	WesternBright ECL HRP substrate	K-12045-D50

2.1.4. Solutions used in Western Blotting

REAGENT NAME		
PHOSPHATE BUFFERED SALINE (PH = 7.4)	137 mM	NaCl
	2.7 mM	KCl
	10 mM	Sodium Phosphate Dibasic
	1.8 mM	Potassium phosphate monobasic
	1 L	ddH_2O
LYSIS BUFFER	1X	Phosphatase Inhibitor (Stock = 100X)
	1X	Protease Inhibitor (Stock = 100X)
	1 µM	DTT (Stock = 1 M)
	1 mM	Sodium Orthovanadate (Stock = 100 mM)
		Complete volume with RIPA buffer

REAGENT NAME		
UREA LYSIS BUFFER	1 mM	Sodium Floride (NaF) (Stock = 500 mM)
	2.5 mM	Disodium pyrophosphate ($Na_2H_2P_2O_7$)
	1 mM	Sodium Orthovanadate (Na_3VO_4) (Stock = 100 mM)
	1 mM	Beta-glycerol phosphate (Stock = 1 M)
	Up to 10 ml	8 M (4.7 g) urea in 20 mM HEPES (pH = 8)
PBS WITH INHIBITORS FOR UREA LYSIS	1 mM	Sodium Floride (NaF) (Stock = 500 mM)
	1 mM	Sodium Orthovanadate (Na_3VO_4) (Stock = 100 mM)
	10 ml	1X PBS
STACKING GEL BUFFER (PH = 6.8)	60.5 g	Tris-Base
		Adjust pH to 6.8 with HCl
	Up to 1 L	ddH_2O
RESOLVING GEL BUFFER (PH = 8.8)	187 g	Tris-Base
		Adjust pH to 8.8 with HCl
	Up to 1 L	ddH_2O
5% BLOCKING SOLUTION	5 g	milk powder or BSA
	100 ml	1X TBS-T
10X TBS (PH = 7.4)	80 g	NaCl
	2 g	KCl
	30 g	Tris-Base
		Adjust pH to 7.4 with HCl
	1 L	ddH_2O

1X TBS-T	100 ml	10X TBS
	1 ml	Tween-20
	Up to 1 L	ddH_2O
10X RUNNNING BUFFER	30 g	Tris-Base
	144 g	Glycine
	10 g	SDS
	Up to 1 L	ddH_2O
10X TRANSFER BUFFER	30 g	Tris-Base
	144 g	Glycine
	Up to 1 L	ddH_2O
SAMPLE LOADING DYE	9 Unit	Beta mercaptoethanol
	1 Unit	Laemli buffer (Stock = 4X)
PRIMARY ANTIBODY (FOR 1:1000 DILUTION)	1X	Sodium Azide (Stock = 100X)
	0.15 g	BSA
	5 ml	TBS-T
	5 µl	Antibody
SECONDARY AB (1:5000 DILUTION)	0.15 g	BSA
	5 ml	TBS-T
	1 µl	Secondary Antibody

2.1.5. Antibodies

	Brand	Catalog No
Jak1	Cell Signaling Technologies	50996
Phospho-Jak1 (Tyr1022)	St John's Laboratory	STJ90314
STAT1	Cell Signaling Technologies	9172
Phospho-Stat1 (Tyr701)	Cell Signaling Technologies	9167
AKT1	Biolegend	680302
Phospho-Akt (Ser473)	Cell Signaling Technologies	9271
ß-Actin	Sigma (Merck)	66009
GAPDH	Santa Cruz	SC-47724
Cleaved Caspase 3	Cell Signaling Technologies	9661
Cleaved Caspase 7	Cell Signaling Technologies	8438
Cleaved Parp	Cell Signaling Technologies	5625
Goat-anti-mouse IgG (H+L), HRP conjugate	Advansta	R-05071
Goat-anti-rabbit IgG (H+L), HRP conjugate	Advansta	R-05072

2.1.6. Solutions and Materials Used in Zebrafish and PIP3 Biosensor Experiments

REAGENT NAME		
E3 MEDIUM	4.91 mM	NaCl
	0.17 mM	KCl
	0.33 mM	$CaCl_2.2H_2O$
	0.33 mM	$MgSO_4.7H_2O$
		Methylene Blue
	Up to 1 L	ddH_2O
4% PFA	4 g	Paraformaldehyde
	100 ml	1X PBS

Product Name	Brand	Catalog No
Mountant with DNA Stain DAPI	P36931	Thermo Fisher

2.2. METHODS

2.2.1. Cell Culture: Maintenance

All cell lines were maintained at 5% CO_2 incubator at 37°C. Passaging of cells were performed when cells reach 90% confluency. For the maintenance of cells following growth media recipes were used.

Table 2. 1. Growth media recipes of cell lines

Mahlavu	10% FBS, 1% Non-Essential Amino Acids, 1% Pen-Strep, completed with High Glucose DMEM
SNU475	10% FBS, 1% Non-Essential Amino Acids, 1% Pen-Strep, completed with High Glucose DMEM
DU145	8% FBS, 1% Pen-Strep, completed with RPMI-1640
C4-2	8% FBS, 1% Pen-Strep, completed with RPMI-1640
PC3	8% FBS, 1% Pen-Strep, completed with RPMI-1640
T47D	4 µg/ml insulin, 2 mM L-glutamine, 1X Non-Essential amino acids, 8% FBS, completed with High Glucose DMEM
MDA-MB-231	10% FBS, 1% Non-Essential Amino Acids, 1% Pen-Strep, completed with High Glucose DMEM
hTERT-RPE1	10% FBS, 1% Pen-Strep, completed with F12/DMEM
MCF10A	4% FBS, 2 mM L-Glutamine, 0.01ng/mL EGF, 25 ng/mL hydrocortisone, 0.01 mg/mL insulin, 1% Pen-Strep, completed with F12/DMEM
MEF	10% FBS, 1% Pen-Strep, completed with High Glucose DMEM

2.2.2. Cell Culture: Thawing

For the thawing of the cells, vial stored in liquid nitrogen was submerged into 37 °C water bath without immersing the cap of vial. Thawing in the water bath needs to be rapid as much as possible to preserve cell viability. Content in the vial was transferred to 15 ml falcon containing 5 ml thawing media to dilute DMSO. Falcon was centrifuged at 1500 rpm for 5 minutes. Supernatant is removed through aspiration. Cell pellet was resuspended in 5 ml thawing media and plated into 6 cm plate. For the preparation of thawing media, only pen-strep is excluded from growth media recipe.

2.2.3. Cell Culture: Passaging

For the passaging of cells, they were first observed under microscope to check confluency and health of cells. Plate to be passaged was washed with 5 ml PBS which was then aspirated. 1 ml of trypsin for 10 cm plate was added to detach cells. For activation of trypsin, plate was placed into incubator for 5 minutes. For Mahlavu, SNU475, PC3, T47D, MDA-MB-231 and MEF cells concentrated (0.25%) trypsin was used. For DU145, C4-2, hTERT-RPE1, and MCF10A cells 0.05% trypsin was used. To inactivate trypsinization approximately 4 ml of growth media was added and cells in the plate were transferred to 15 ml falcon. Falcon was centrifuged at 1500 rpm for 5 minutes. Supernatant was aspirated and resuspended in fresh growth media. 9 ml of fresh growth media was added to new 10 cm plate and calculated volume of cell suspension was added. For Mahlavu cells 1/10 or 1/12; for SNU475, DU145, PC3, MDA-MB-231, hTERT-RPE1, MCF10A, and MEF cells 1/8 or 1/10; for C4-2 cells 1/4; for T47D cells 1/3 dilution was performed depending on initial confluency.

2.2.4. Cell Culture: Freezing

For freezing of cells, plate with 70 – 80% confluency is desired. Cells were washed with PBS. 1 ml of trypsin was added for 10 cm plate. Plate was incubated for 5 minutes at 37 °C. trypsin was inactivated with addition of 4 ml of growth media. Content in the plate was transferred to 15 ml falcon which was centrifuged for 5 minutes at 1500 rpm. Supernatant was removed and cell pellet was resuspended in freezing media. Freezing media was prepared as 10% DMSO, 50% FBS, 40% basal media (Depending on cell type DMEM, RPMI-1640 or F12/DMEM etc. can be used.) 2 or 3 vials with 1 ml cell suspension each were frozen from a single 10 cm plate based on confluency of the cells. vials were placed into Mr. Frosty which was then placed into -80°C freezer overnight. For permanent storage of cells liquid nitrogen tank (-196 °C) was used.

2.2.5. Sulforhodamine B Assay (SRB)

For SRB assay 96-well plates whose peripheral wells were filled with 1X sterile PBS beforehand was used. To seed cells into 96-well plate cells were counted using hemocytometer. Cell suspension containing required number of cells for a single 96-well plate is prepared. From this suspension 100 µl containing desired number of cells per well is seeded. For Mahlavu, SNU475, MDA-MB-231, PC3, DU145, hTERT-RPE1 and MCF10A 2000 cells per well were seeded. For C4-2 10000 cells per well were seeded. For T47D 3000 cells per well were seeded. For MEF 1500 cells were seeded. After seeding, cells were grown for 2 days in regular growth media. Then, compound treatments were performed with 0.3, 0.75, 1.5, 3, 6, 10 µM of each compound. All cell lines were treated with equimolar concentrations of compounds. Compound treatments were prepared in 100 ul (per well) of regular growth media in a way that they contain 2 times more concentrated compounds than desired. Because of the presence of 100 µl of growth media in the

wells before compound treatment, compounds were prepared as 2X which were diluted by half afterwards. Cells were treated with compounds with indicated concentrations for 3 days. At the end of 3 days long compound treatment, Sulforhodamine B assay protocol starts. Media on top of the cells were discarded gently considering the detachment of cells. Cells were fixed with 10% TCA (50 µl per well) for 1 hour at +4°C or overnight. After fixation period ends, cells were washed with dH_2O 5 times to remove fixation solution. Cells were stained with 0.4% SRB dye (50 µl per well) for 30 minutes in the dark at room temperature. To get rid of SRB dye, cells were washed with 1% acetic acid until all dyes were removed. After removing dyes completely, cells were left for airdry overnight or for a couple of hours, then plates were scanned using scanner. To quantify cell viability, cells were de-stained with 150 µl of 10 mM non buffered tris-base and shaken on the shaker until obtaining homogenous appearance of dye. Measurements of optical density were taken at 564 nm.

2.2.6. Western Blot: Cell Seeding & Treatment

Western blot analysis was performed for biochemical characterization of apoptosis and signaling pathways modulated after 24- and 48-hour treatments. For these experiments, cells were seeded in low density so that they don't reach confluency at the end of compound treatment period. All cells except for C4-2 were seeded the day before compound treatment. C4-2 cells were seeded 2 days before compound treatment. At the day of compound treatment calculated volume of compounds were given to 10 cm plates. Cells were incubated with compounds either for 24- or 48-hour. At the end of treatment, cells were collected by scraping.

2.2.7. Western Blot: Harvest and Lysis

Cells were washed with 1X PBS in order to get rid of dead cells and remaining media. PBS was aspirated. For 10-cm plate 2-3 ml of 1X ice cold-PBS was added and within PBS cells were scraped on ice and transferred to 15-ml falcon tubes. Cells were centrifuged for 8 minutes at 1500g at +4°C. Supernatant was removed, cell pellet was snap frozen and stored at -80°C.

Lysis buffer was prepared according to recipe found in materials section and kept on ince. Volume of lysis buffer was arranged according to total volume of cell pellets. Prepared lysis buffers were distributed to each cell pellet (1:1 ratio of pellet/lysis buffer) and incubated for 30 minutes on ice. Every 10 mins tubes were flicked without pipetting. At the end of incubation, tubes were centrifuged at 15000g for 15 minutes at +4°C. supernatant containing protein lysate was snap frozen and stored at -80°C.

For the lysis of treated C4-2 cells, urea-based lysis method was preferred. Cells were washed 3 times with 1X ice cold PBS with inhibitors (recipe can be found in materials section). Cells were scraped within urea lysis buffer on ice (recipe can be found in materials section). Cell suspensions were sonicated at 40% amplitude for 15 seconds 4 times with 25 seconds resting between each sonification. Then, protein lysates were obtained after centrifuging at 14000 rpm for 20 minutes at 4°C. Supernatants containing protein were snap frozen and stored at -80°C.

2.2.8. Western Blot: BCA and Sample Preparation

Commercial BCA kit was used to quantify concentration of proteins. Protein lysates were diluted 25 times by mixing 24 µl of ddH_2O with 1 µl protein sample to save on protein lysate (for a single well of 96 well plate). Accordingly, BSA standards were dilutes as well. As recommended by the manufacturer, working solution was prepared as 50:1 ratio of solution A: B and 200 µl of this

solution was distributed to each well. Plate was incubated at 37°C for 30 minutes and absorbances were obtained with plate-reader.

After calculating concentration of proteins,15-25 µg containing protein volume was mixed with loading dye. Final volume was brought to 15-25 µl with ddH_2O. Loading dye was prepared by mixing beta-mercaptoethanol with 4X laemli buffer in 1:9 ratio. Prepared samples were boiled at 95 °C for 5 minutes. If needed they were stored at -20°C or used immediately after warming.

2.2.9. SDS-PAGE and Western Blotting

Usually, 10% SDS-PAGE gel was prepared. For 10% resolving gel preparation (10 ml), 3.3 ml acrylamide/bisacrylamide (30% w/v), 4.1 ml ddH2O, 2.5 ml resolving buffer, 50 µl 10% APS, 5 µl TEMED were mixed. For 4% stacking gel preparation (5 ml) 0.66 ml acrylamide/bisacrylamide (30% w/v), 3 ml ddH2O, 1.26 ml resolving buffer, 25 µl 10% APS, 5 µl TEMED were mixed While preparing gels according recipe, 10% APS and TEMED were added lastly to prevent premature polymerization of gels. Using 1.5 mm spacers and combs, western blot casting was performed. 10% resolving gel solution was poured initially and coated with isopropanol. After solidifying 4% stacking gel solution was poured and comb was placed. After stacking gel becomes solidified, SDS-PAGE is ready for use.

Running of western blot was performed at 100V and 90-100 minutes approximately but until dye passed the stacking gel part, running was done at 80V. After clear separation protein ladder, transfer was performed through wet transfer in ice. Proteins were transferred to nitrocellulose membrane and power supplier was set to 250 mA – 150 minutes. After transfer finishes, nitrocellulose membrane was stained with Ponceau S to see efficiency of protein transfer. Membranes were cut

according to molecular weight of protein of interest. Then, they are blocked with 5% milk or BSA for 1 hour at room temperature. Overnight incubation with primary antibodies was done. Next day, membranes were washed with TBS-T for 5 minutes 3 times and incubated with secondary antibodies for 1 hour at room temperature. Then, membranes were again washed with TBS-T for 5 minutes 3 times. Proteins were imaged using ECL kit.

2.2.10. PIP3 Biosensor Assay

C4-2 cells already transfected with GFP-PH^{BTK} construct were used in this experiment. 350.000 GFP-PH^{BTK} expressing C4-2 cells were seeded per well to 6-well plate. Before seeding sterile coverslips were placed to each well. The next day, cells were treated with 5 µM EB38, 5 µM C160, and 3 µM GDC0941 for 6h. at the end of treatment period, cells were washed with 1X PBS. Fixation of cells were performed with 4% PFA in 1X PBS for 15 minutes at room temperature. After fixation ends, wells were washed with 1X PBS 3 times. Then, coverslips were removed considering which side of the coverslip has cells and dipped into ddH_2O for washing. Excess water was eliminated. Coverslips were mounted onto drop of (˜10 µl) mountant with DAPI and incubated overnight at room temperature in the dark. Next day, images of cells were obtained with fluorescence microscopy.

2.2.11. Molecular Docking Analysis

Avogadro tool was used to reveal the 3D structures of the compounds since they are no available crystal structures of compounds. Optimize Geometry Function was selected to identify the most optimal conformations using 3D structures generated with Build function. Then, Conformer Search function was used to provide the best conformations (Systemic rotor search option was

selected). The polar hydrogens of the ligands were added in AutoDock Tools. Ligands were determined as flexible while kinase models are rigid. The co-crystalized ligands on the JAK1 models were eliminated from the structure using PyMOL. GridBox function was utilized to determine docking area. Locations of gridbox were determined based on the location of catalytic site that is bound with co-crystalized ligand previously. The number of modes was decided as 10. PDBQT files were constituted with AutoDock Tools utility scripts. AutoDock Vina software was utilized to do docking analyses. RMSD cutoff was determined as 2 Å.

2.2.12. Spheroid Growth Inhibition

In order to grow spheroids special, custom-built platform was utilized. A customized mold was used to generate platform with 24 micron-sized wells. Each platform can fit into single well of 96-well plate. 400 C4-2 cells were seeded per well. After tight spheroids were formed, which approximately takes 3 days, treatment with compounds were performed. Growth media of C4-2 spheroids were replaced with inhibitory media containing 0.75, 1.5, 3, 5, and 10 μM of compounds. Spheroids were treated with compounds for 3 days. At the end of experiment, individual spheroid sizes were analyzed.

2.2.13. Zebrafish Husbandry and Toxicity Test

Adult zebrafish were maintained in 27±1°C circulating water system with 14 h light / 10 h dark periods. Fertilization was achieved by placing adult zebrafish in a breeding tank with 1:2 male – female ratio. Male and female zebrafish were separated overnight and separator was removed in the morning to initiate fertilization. Resulting embryos were incubated in 10 cm petri dish with E3 media in 28°C incubator. At 2 dpf, zebrafish larvae were used for toxicity experiment. For the

conduction zebrafish toxicity experiments, 2 dpf wild type AB strain zebrafish were distributed to 48 well plate in a way that each well receives 6 zebrafish (n = 18 for each group). Treatment of zebrafish larvae was performed from 2 dpf to 5 dpf. To test toxicity of low concentrations zebrafish were treated with 2, 5, and 10 μM of each compound and biotin. To test toxicity of high concentrations zebrafish were treated with 10, 30, and 50 μM of each compound and biotin. E3 media in which zebrafish grow renewed daily along with renewal of treatments. At the end of experiment, zebrafish were anesthetized with 0.04% tricaine (MS-222) to record images of morphology of zebrafish. Images of zebrafish were obtained on 3% methylcellulose.

2.2.14. Free Biotin Competition Assay

On the first day DU145 cells were seeded into 96-well plate. The next day, 30 min prior to compound treatment, DU145 cells were incubated with biotin with the indicated concentrations. Then, compound treatment was performed with IC50 values of DU145. For the EB38 10 μM, for C160 2 μM, and for C161 2.5 μM was used. Biotin concentrations were renewed daily. At the end of 2 days, experiment was ended and SRB assay was conducted to measure viability of the cells.

2.2.15. Statistical Analysis and Determination of IC50

GraphPad 10 was used to calculate IC50 values for cell lines. Blank-corrected data was used and concentration of drugs were transformed according to X = log(X) formula and normalization of data was done. Non-linear regression (curve fit) model was selected. IC50 curves were drawn with Log (inhibitor) vs. normalized response – Variable slope equation. All statistical analyses were performed using GraphPad 10. Two-way ANOVA and one-way ANOVA followed by multiple comparison tests were done. (ns > p 0.05; * $p < 0.05$; ** $p < 0.01$; *** $p < 0.001$; **** $p < 0.0001$)

3. RESULTS

3.1. Assessment of Cytotoxicity of Parental EB38 and Its Biotinylated Derivatives

EB38 is a vicinal diaryl substituted isoxazole derivative, which was shown to have antiproliferative effects on breast cancer (MCF7, MDA-MB231) and liver cancer (Huh7, mahlavu), induce apoptotic cell death, and inhibit growth of xenograft of breast and liver cancer previously by Sümeyye et al (Turanlı et al., 2022). Building upon these findings where antitumorigenic efficiency of EB38 was elucidated, compound160 (C160) and compound161 (C161) are synthesized as derivatives of parental compound, EB38. While compound 160 is single biotinylated derivative of EB38, compound 161 is the PEG-biotin conjugated derivative of EB38. Biotinylated derivatives of EB38 allowed us to study contribution of biotin conjugation to efficacy of antitumorigenic capacity of drugs.

A panel of cancer cell lines were tested with SRB assay to evaluate the antiproliferative potency of EB38 and its biotinylated derivatives in order to investigate impact of biotin conjugation. In this panel, we incorporated Mahlavu and SNU475 cells as liver cancer models; C4-2, DU145, and PC3 as prostate cancer models; MDA-MB-231, and T47D as breast cancer models. Mahlavu is a poorly differentiated and aggressive hepatocellular carcinoma cell line (Keskin et al., 2013) with p53 mutation (Puisieux et al., 1993). Similar to Mahlavu cells, SNU475 cells are HCC with p53 mutation (Kang et al., 1996). MDA-MB-231 is triple negative breast cancer, lacking the expression of PR, ER, and HER2 receptor. It has mutated p53 (Hui et al., 2006) and exhibits aggressive, invasive, and metastatic characteristics (Huang et al., 2020). T47D belongs to class of luminal A breast cancer, with ER and PR positive but HER2 negative expression. It is frequently used in hormone therapy research (Yu et al., 2017). PC3 (H. Wang

et al., 2023) and C4-2 (Gan et al., 2009) are castration resistant (CRPC) and PTEN-null cell lines while DU145 is a castration resistant PTEN-wt cell line (Fraser et al., 2011). We aimed to include cancers with different molecular characteristics to assess tumorigenic capacity of EB38 and its derivatives on broad range of cancer types. Cancer cells were treated with equimolar doses of compounds to evaluate their efficacies comparatively. In all cell lines tested, biotinylated derivatives, C160 and C161, inhibited proliferation of cancer cells more efficiently compared to EB38. Differences in the growth inhibition capacity of compounds are more pronounced particularly in low concentrations (Figure 3.1).

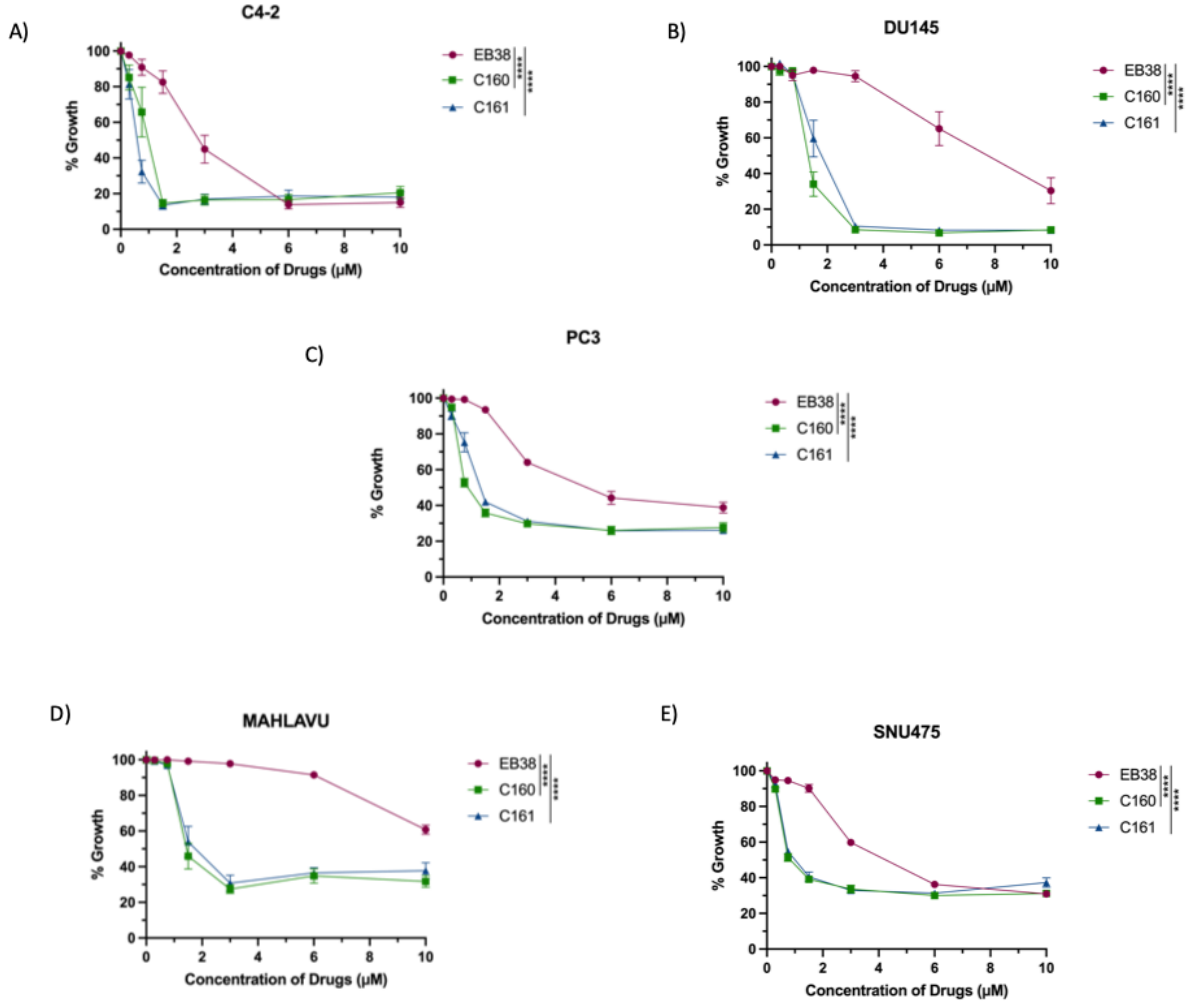

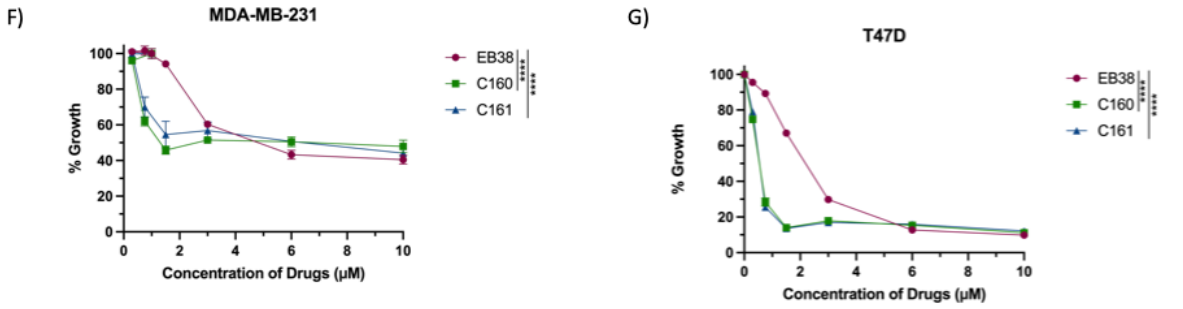

Figure 3. 1. Biotinylated compounds exhibit broad – range antiproliferative activity in multiple cancer cell lines. Cellular growth was assessed using Sulforhodamine B (SRB) assay on cancer cell lines treated with compounds for 72h with the varying concentrations. Dose – growth response graphs were drawn for A) C4-2, B) DU145, C) PC3, D) Mahlavu, E) SNU475, F) MDA-MB-231, G) T47D. Experiments were performed in triple technical replicates. Absorbance values are normalized to DMSO- treated controls. For C4-2, DU145, and Mahlavu n = 3. For PC3, SNU475, MDA-MB-231, and T47D n = 4. Statistical analysis was performed by two-way ANOVA followed by Tukey's multiple comparisons test. Error bars represent SEM. * $p < 0.05$; ** $p < 0.01$; *** $p < 0.001$; **** $p < 0.0001$

These results demonstrate that all compounds are able to suppress proliferation of cancer cells, with biotinylated derivatives halting growth more potently. Growth inhibition of compounds is also reflected on IC50 values. Biotinylated derivatives resulted in lower IC50 values in all cancer lines (Table 3.1).

Table 3. 1. IC50 Values of Different Cancer Cell Lines (μM)

Cell Line	EB38	C160	C161
C4-2	3.1	1.1	0.7
DU145	7.5	1.3	1.7
PC3	5.7	1.3	1.7
MAHLAVU	11.3	2.4	2.9
SNU475	4.6	1.4	1.6
MDA-MB-231	5.3	3.9	4.6
T47D	2.1	0.5	0.5

In addition to cancer cell lines, compounds are tested in non-tumorigenic cell lines as well. Although these cell lines are known to be non-tumorigenic, they are still considered highly proliferative and immortalized. Moreover, regarding them as true representation of healthy cells may not be adequate. To test capacity of compounds on highly proliferative cell lines, hTERT-RPE1, MCF10A, and MEF cells are utilized. In these cell lines, EB38 halted growth of cells to a lesser extent compared to biotinylated derivatives, highlighting the enhanced cytotoxic ability of biotinylated compounds in highly proliferative cells as well (Figure 3.2).

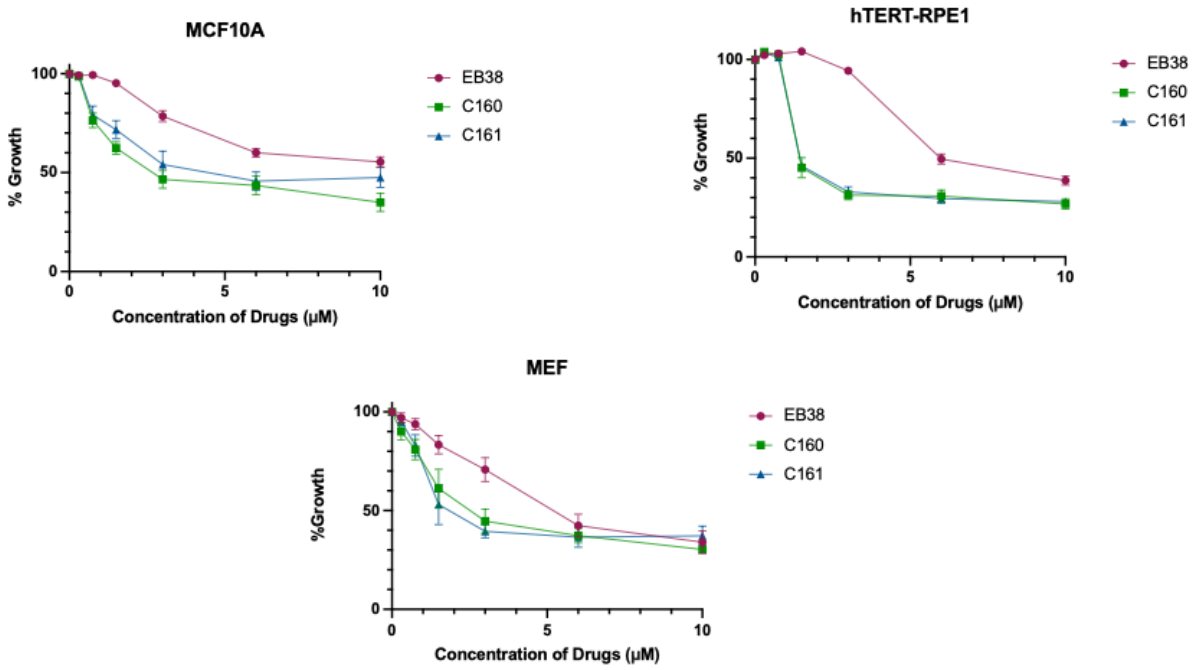

Figure 3. 2. Biotinylated compounds exhibit anti-growth activity in highly proliferative normal cell lines. Cellular growth was assessed using Sulforhodamine B (SRB) assay on healthy cell lines treated with compounds for 72h with the varying concentrations. Dose – growth response graphs were drawn for A) MCF10A, B) hTERT-RPE1, C) MEF. Experiments were performed in triple technical replicates. Absorbance values are normalized to DMSO-treated controls. For MCF10A n = 5. For hTERT-RPE1 and MEF n = 3. Statistical analysis was performed by two-way ANOVA followed by Tukey's multiple comparisons test. Error bars represent SEM. * $p < 0.05$; ** $p < 0.01$; *** $p < 0.001$; **** $p < 0.0001$

Although EB38 and its derivatives suppress growth of non-tumorigenic cells, when IC50 values of healthy cells were investigated to make quantitative comparisons with cancer cells, IC50 values of cancer cell lines are slightly lower than healthy cells (Table 3.2).

Table 3. 2. IC50 Values of Different Healthy Cell Lines (μM)

Cell Line	EB38	C160	C161
MCF10A	10.4	3.7	5.8
hTERT-RPE1	6.8	2.2	2.2
MEF	5.7	2.9	3.2

3.2. Characterization of Proapoptotic Capacity of EB38 and Its Biotinylated Derivatives

After establishing anti-proliferative capacity of EB38 and its biotinylated derivatives, we moved to characterize pro-apoptotic properties of compounds. For this reason, Mahlavu cells were treated for 24 hours with 1 μM and 5 μM concentrations of EB38 and C160-C161 as low and high doses. We demonstrated that both EB38 and C160-C161 induced apoptotic cell death in liver cancer as reflected on cleavage of PARP, caspase 3, and caspase 7 (Figure 3.3). When EB38 and C160 are compared, induction of apoptosis was achievable with low doses of C160-C161 while EB38 induces apoptotic cell-death with high doses only. Additionally, we included DU145 and C4-2 cells in our experiments to expand our understanding of apoptotic activities of compounds on different cancer cells. We demonstrated that 24 hours is sufficient to induce apoptosis by the compounds. Moreover, prostate cancer (C4-2 and DU145) and liver cancer (Mahlavu) cell lines are responsive towards both EB38 and its biotinylated compounds, with C160 and C161 treatment inducing augmented apoptotic cell death with lower doses.

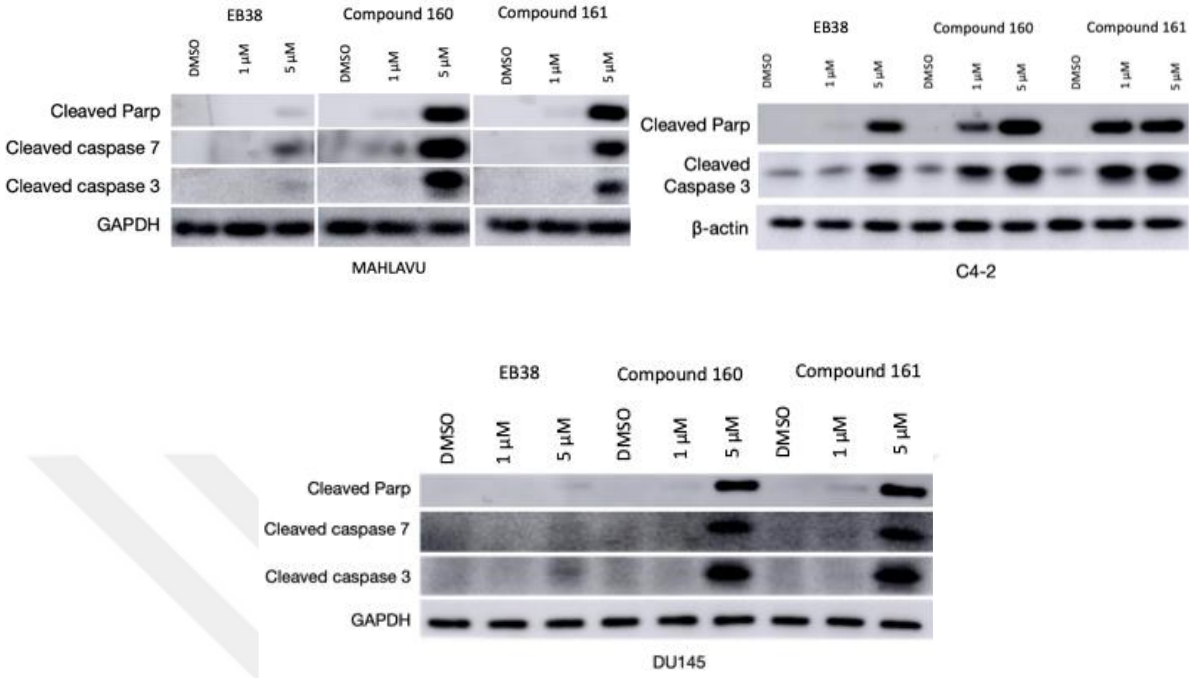

Figure 3. 3. Biotinylated compounds induce augmented activation of proapoptotic pathways in liver and prostate cancer in 24-hour treatment. Western blot analysis was performed against cleaved PARP, cleaved caspase 3, and cleaved caspase 7 for Mahlavu, DU145, and C4-2 cells that were treated with low and high doses of compounds for 24h. Experiments were performed in two biological replicates.

3.3. EB38 and Its Biotinylated Derivatives Exert Their Anti-Tumorigenic Properties Through JAK/STAT Pathway

Despite promising results where EB38 and biotinylated compounds were characterized for its antigrowth and proapoptotic capacity, molecular mechanism of action of EB38 and its biotinylated derivatives remains unelaborated. To address this gap, we first concentrated on dissecting the signaling pathways that are potentially modulated by EB38 and its biotinylated derivatives. We started with conducting western blot analysis against JAK/STAT and PI3K

oncogenic pathways which are commonly dysregulated in cancer and play essential roles in growth, survival, and immunity.

First, to examine long-term consequences of compound treatment we treated Mahlavu cells with EB38 and its biotinylated derivative (C160) for 48 hours with 1 μM and 5 μM (Figure 3.4). This prolonged treatment duration was chosen to elaborate on possible long-term impacts on protein expression and activation status, which may indicate sustained inhibition of cellular responses. With the treatment of EB38 and C160, we detected inhibition of phosphorylation of JAK1, STAT1, and AKT, which may reflect inhibition of JAK/STAT and PI3K signaling pathways. Interestingly, total protein level of JAK1, STAT1, and AKT was also downregulated upon compound treatments. Reduction of total protein levels may suggest effects on compounds on regulation of protein turnover and degradation. When EB38 and C160 are compared we observed that inhibition was potentiated with C160 treatment. Comparing equimolar concentrations of EB38 and C160, we observed that C160 resulted in more significant downregulation of phosphorylation of JAK1 (Tyr1022), STAT1 (Tyr701), and AKT (Ser473).

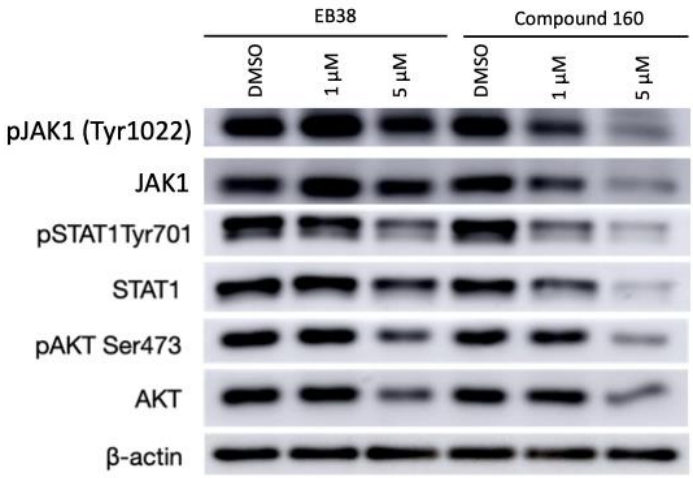

Figure 3. 4. EB38 and its biotinylated derivatives modulate JAK/STAT pathway together with PI3K pathway in the long-term inhibition. Western blot analysis was conducted with antibodies targeting p-JAK1 (Tyr1022), p-STAT1 (Tyr701), p-AKT(Ser473), JAK1, STAT1, and AKT for Mahlavu cells that were treated with low (1 µM) and high doses of compounds for 48h. Experiments were performed in two biological replicates.

After observing inhibition of both PI3K and JAK/STAT pathways in the long term, we decided to investigate whether PI3K pathway is direct target of EB38 and biotinylated C160. For this aim, we utilized PIP3 biosensor approach frequently used in our research group, which indicates activation of PI3K pathway. In this biosensor we have PH domain of BTK (Bruton's Tyrosine Kinase) tagged with GFP. When PI3K pathway is activated, PIP2 lipid species are phosphorylated to PIP3 by PI3K enzyme and PH domain containing proteins such as BTK is recruited to PIP3 species generated in the plasma membrane. In this regard, GFP-PH ^{BTK} is diffused inside the cytoplasm of cells when PI3K is inhibited. When PI3K is active, GFP signals appear to be in cellular membrane. This PH^{BTK}-based biosensor is used for its

advantages including high specificity that allows binding of PH domain selectively to PIP3 generated but not other lipid species, high sensitivity that help capture small changes in PIP3 levels, and minimal basal membrane localization when not active (Várnai et al., 1999).

Here, we treated C4-2 prostate cancer cells expressing PH^{BTK} – GFP construct with EB38, biotinylated C160, and pan-PI3K inhibitor GDC0941 as positive control for 6-hours to capture, if present, initial modulations induced by compounds on PI3K signaling cascade (Figure 3.5). When peripheral GFP signals coming from plasma membrane were quantified, as expected, GDC0941 treatment diminished peripheral signals significantly compared to DMSO control. For the EB38- and C160-treated groups, quantification of peripheral GFP signals didn't reveal any significant differences compared to DMSO-treated group (Figure 3.5). These findings suggest that PI3K signaling pathway may not be the direct target of EB38 and its derivatives as evidenced by no inhibition of PI3K.

A)

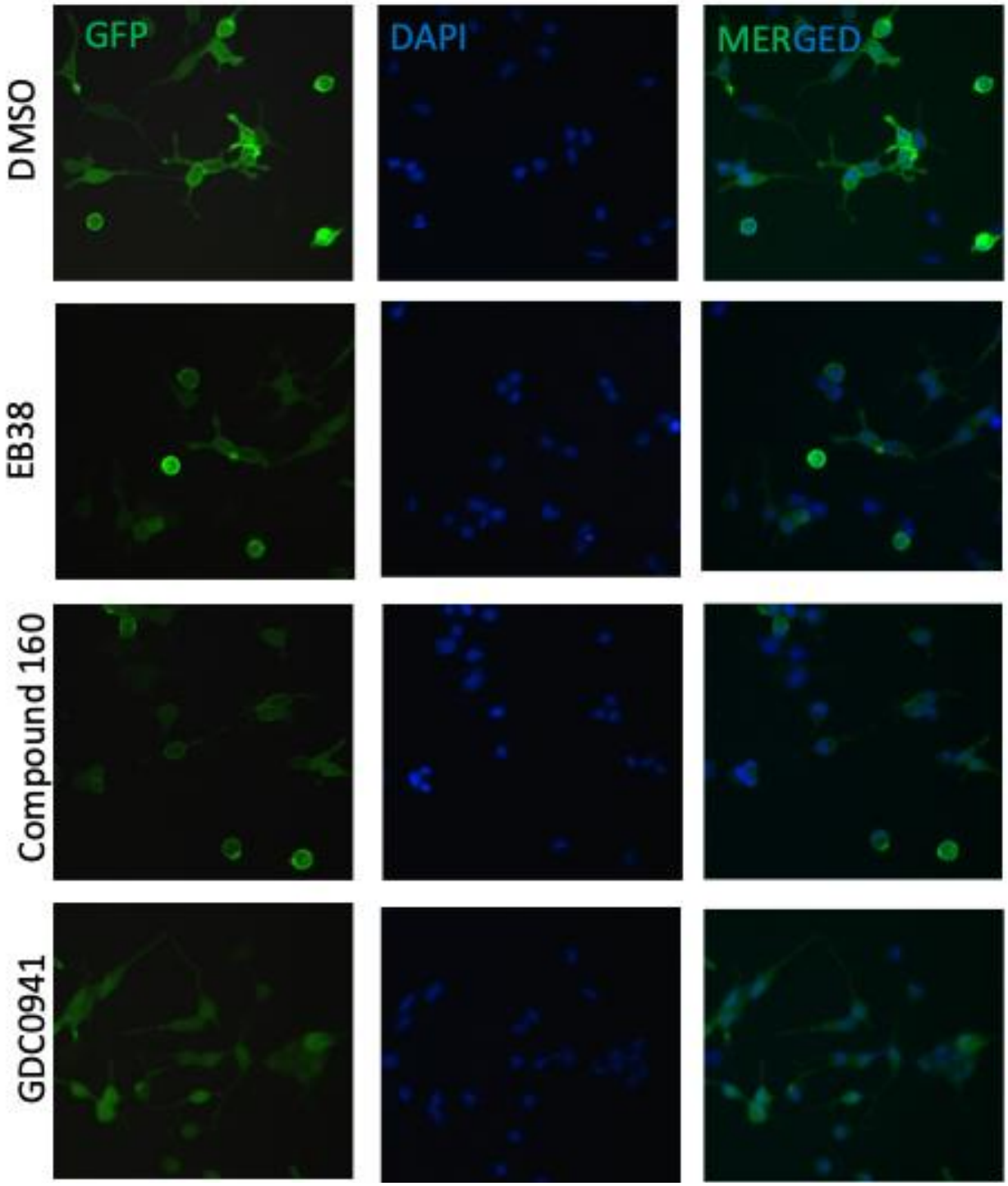

B)

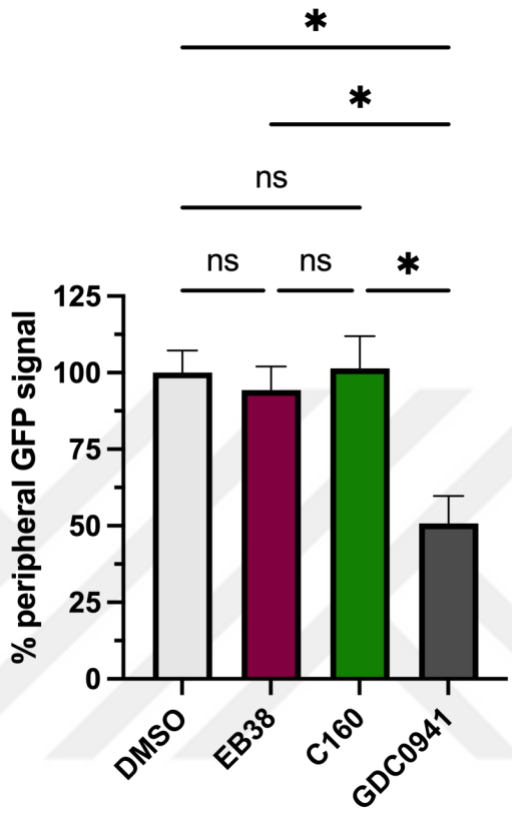

Figure 3. 5. Biotinylated compounds do not primarily modulate PI3K signaling. PH^{BTK} – GFP expressing C4-2 cells were inhibited with compounds and pan PI3K inhibitor GDC-0941 as positive control for 6 hours. A) Representative images of C4-2 cells were given. B) Peripheral GFP signal as a indication of PI3K activation was quantified. Experiments were performed in three biological replicates. Statistical analysis was performed by one-way ANOVA followed by Tukey's multiple comparison tests. Error bars represent SEM. * $p < 0.05$; ** $p < 0.01$; *** $p < 0.001$; **** $p < 0.0001$

After constituting long-term (48h) impacts of EB38 and its biotinylated derivative, we inhibited Mahlavu cells for 24 hours to examine short term effects of EB38 and its derivatives on them. In addition to Mahlavu cells, we expanded the diversity of cell types by including

C4-2 and DU145 cells to assess how broadly effective these compounds are. Similar to the 48-hour inhibition, we treated different cell lines with 1 μM and 5 μM doses of EB38 and its derivatives and performed western blot analysis against p-JAK1 (Tyr1022), p-STAT1 (Tyr701), p-AKT(Ser473), JAK1, STAT1, and AKT (Figure 3.6). We found that in compound-treated DU145 cells, p-JAK1 (Tyr1022) and p-STAT1 (Tyr701) levels are suppressed more pronouncedly compared to p-AKT (S473). Also, inhibition of oncogenic signaling pathways induced by C160 and C161 is more efficient than EB38, demonstrating enhancement of activity of compounds through biotin-conjugation. For the C4-2 cells, we couldn't obtain signal for p-JAK1 and JAK1, which might be due to technical constraints. However, putting JAK1 signals aside, we showed that levels of p-STAT1, which is acting downstream of JAK1, are suppressed with EB38 and more predominantly with its biotinylated derivatives, showing inhibition of JAK/STAT pathway. When we look at levels of p-AKT (S473), we observed that there is no obvious inhibition of PI3K pathway. For the inhibition of oncogenic pathways in Mahlavu cells, we observed that biotin conjugation resulted in enhancement of suppression of JAK/STAT and PI3K pathway (except for p-AKT signal in C161-treated group) compared to non-biotin conjugated EB38. Also, compared to inhibition of PI3K pathway, we observed better inhibition of JAK/STAT pathway.

A)

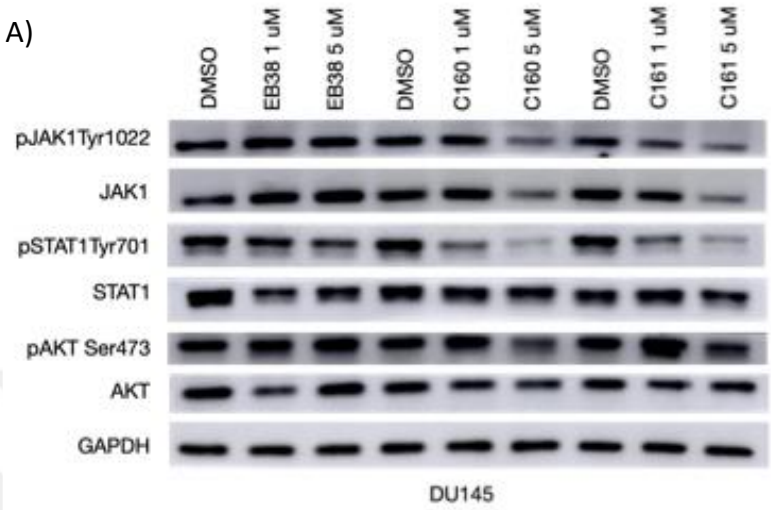
DMSO
EB38 1 uM
EB38 5 uM
DMSO
C160 1 uM
C160 5 uM
DMSO
C161 1 uM
C161 5 uM
pJAK1Tyr1022
JAK1
pSTAT1Tyr701
STAT1
pAKT Ser473
AKT
GAPDH
DU145

B)

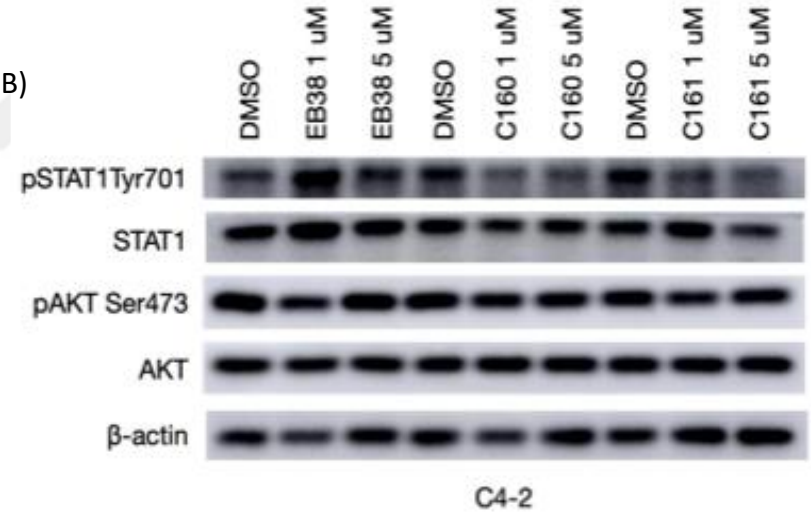
DMSO
EB38 1 uM
EB38 5 uM
DMSO
C160 1 uM
C160 5 uM
DMSO
C161 1 uM
C161 5 uM
pSTAT1Tyr701
STAT1
pAKT Ser473
AKT
β-actin
C4-2

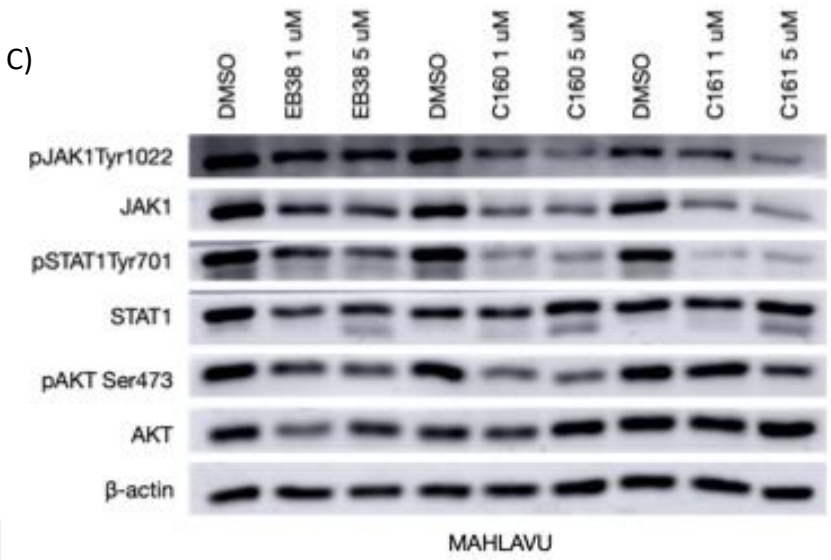

Figure 3. 6. Biotinylated compounds act on JAK/STAT pathway in the short-term inhibition. Western blot analysis was conducted with antibodies targeting p-JAK1 (Tyr1022), p-STAT1 (Tyr701), p-AKT(Ser473), JAK1, STAT1, and AKT for A) Mahlavu, B) DU145, C) C4-2 cells that were treated with low and high doses of compounds for 24h. Experiments were performed in two biological replicates.

These western blot analyses together with PIP3 biosensor experiments suggest that EB38 and biotinylated derivatives act through targeting the same cellular signaling pathways, which is JAK/STAT pathway. We propose that primary target of compounds is JAK/STAT pathway while PI3K pathway is inhibited subsequently as secondary mechanisms by compounds.

To provide more solid support for our hypothesis, we performed computational molecular docking analysis. Here, binding of compounds to catalytic site of JAK1 was investigated using AutoDock Vina tool. For this purpose, compounds were docked to 20 different crystal structures of JAK1 available in PDB. The same molecular docking simulations were performed

for Ruxolitinib, FDA-approved JAK1/2 inhibitor (Ostojic et al., 2011). Ruxolitinib was included as positive control for comparative docking analyses. Mean of binding affinity of Ruxolinitib across 20 structures was calculated to be -8.37 kcal/mol. Therefore, -8 kcal/mol was determined as threshold for high binding affinity. Binding affinities of compounds calculated for each structure were given in Figure 3.7.

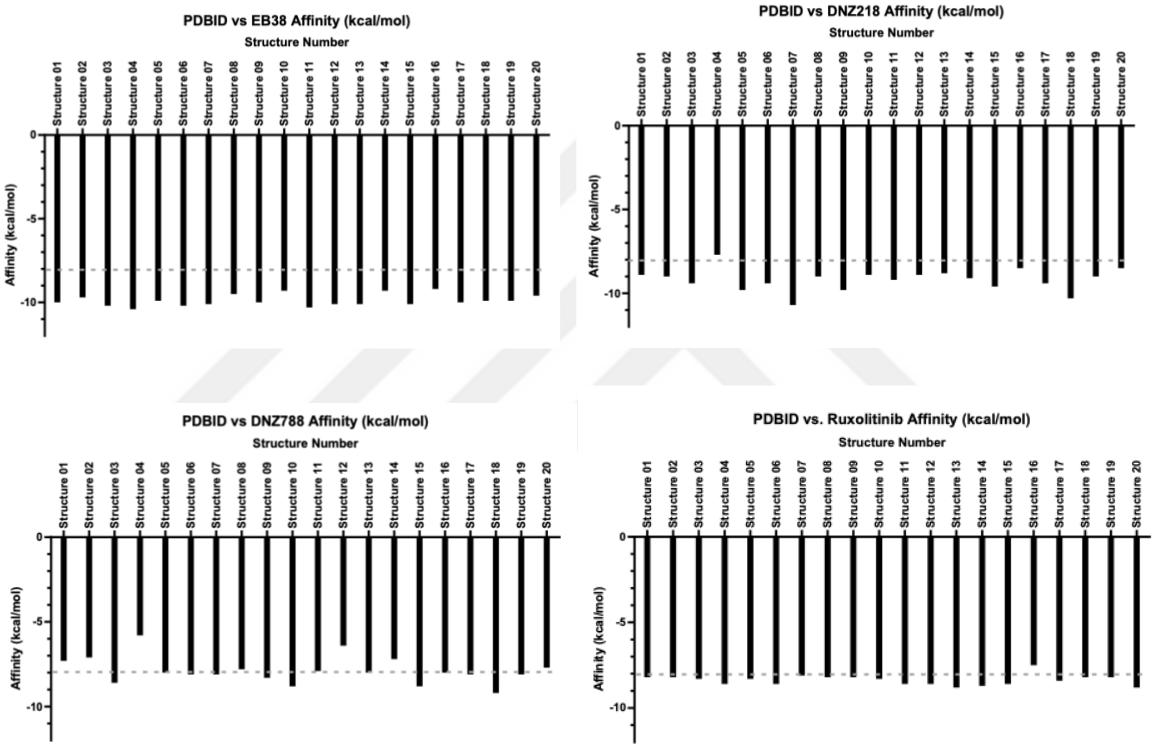

Figure 3. 7. Binding affinities of EB38 and its biotinylated derivatives for JAK1 catalytic site. Each compound was docked to crystal structures available in PDB. Ruxolitinib was included as positive control. Gray dashed line represents mean binding affinity of Ruxolitinib (-8.37 kcal/mol) across 20 structures. (DNZ218 = C160, DNZ788 = C161). Docking analyses were performed by Hazal Beril Çatalak Yılmaz.

EB38 and C160 resulted in consistent high binding affinities towards JAK1 catalytic site that are comparable to binding affinity of Ruxolitinib. However, binding affinity of C161 for JAK1 is

relatively variable compared to EB38, C160, and Ruxolitinib. Mean binding affinity of C161 is calculated to be -7.86 kcal/mol. The reason for variable binding affinity of C161 towards JAK1 catalytic site can be due to its large size and greater conformational flexibility of side chains that increase possibility of steric hinderance and obstruct stable binding. These findings suggest that EB38 and its derivatives target catalytic site of JAK1 enzyme efficiently, comparable to FDA-approved JAK1 inhibitor.

3.4. Investigating the Potential Mechanisms of Enhanced Uptake of Biotinylated Compounds

In the literature there are studies that propose SMVT transporters carry out uptake of biotin conjugated compounds while other studies suggest the involvement of alternative mechanism such as receptor-mediated endocytosis. To this end, we conducted free biotin experiment with DU145 to understand what mediates more enhanced antitumorigenic capacity of our biotinylated compounds. We hypothesized that if the C160 and C161 accumulate in the cells through SMVTs, their uptake will be diminished in the presence of biotin which saturates SMVTs and we will observe increased viability while uptake of EB38 remains unaffected. We treated DU145 cells with IC50 doses of EB38, C160, and C161. Before treating the cells with compounds, we started biotin exposure so that transporters get saturated with free biotin. At the end of this experiment, we observed that with the increasing concentration of biotin, there is no improvement in the cellular viability of either C160- or C161-tretaed DU145 cells (Figure 3.8). This suggests that biotinylated compounds might be taken into cells through mechanism that are not saturable with biotin treatment such as endocytosis which enables large-scale uptake.

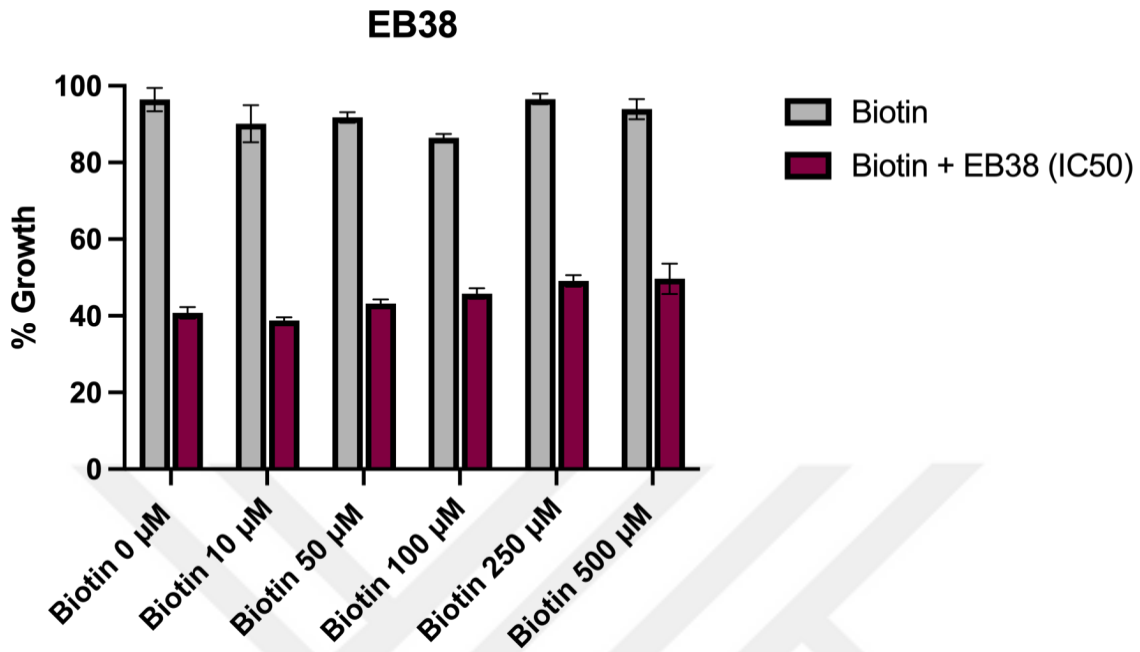
EB38
% Growth
100
80
60
40
20
0
Biotin 0 µM
Biotin 10 µM
Biotin 50 µM
Biotin 100 µM
Biotin 250 µM
Biotin 500 µM
Biotin
Biotin + EB38 (IC50)

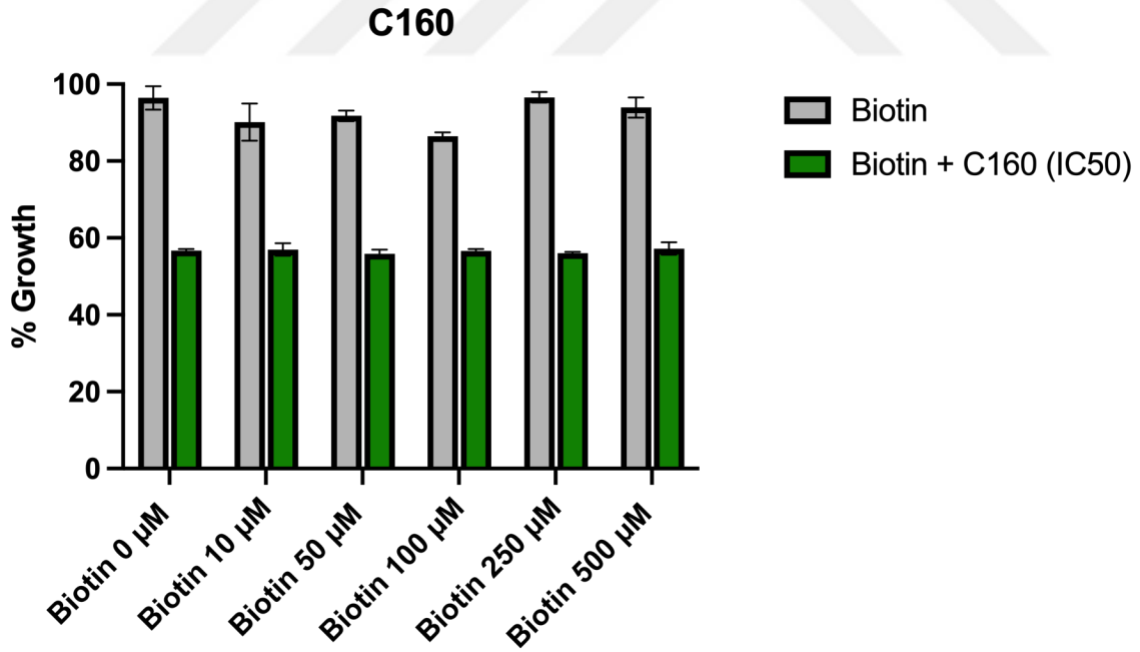
C160
% Growth
100
80
60
40
20
0
Biotin 0 µM
Biotin 10 µM
Biotin 50 µM
Biotin 100 µM
Biotin 250 µM
Biotin 500 µM
Biotin
Biotin + C160 (IC50)

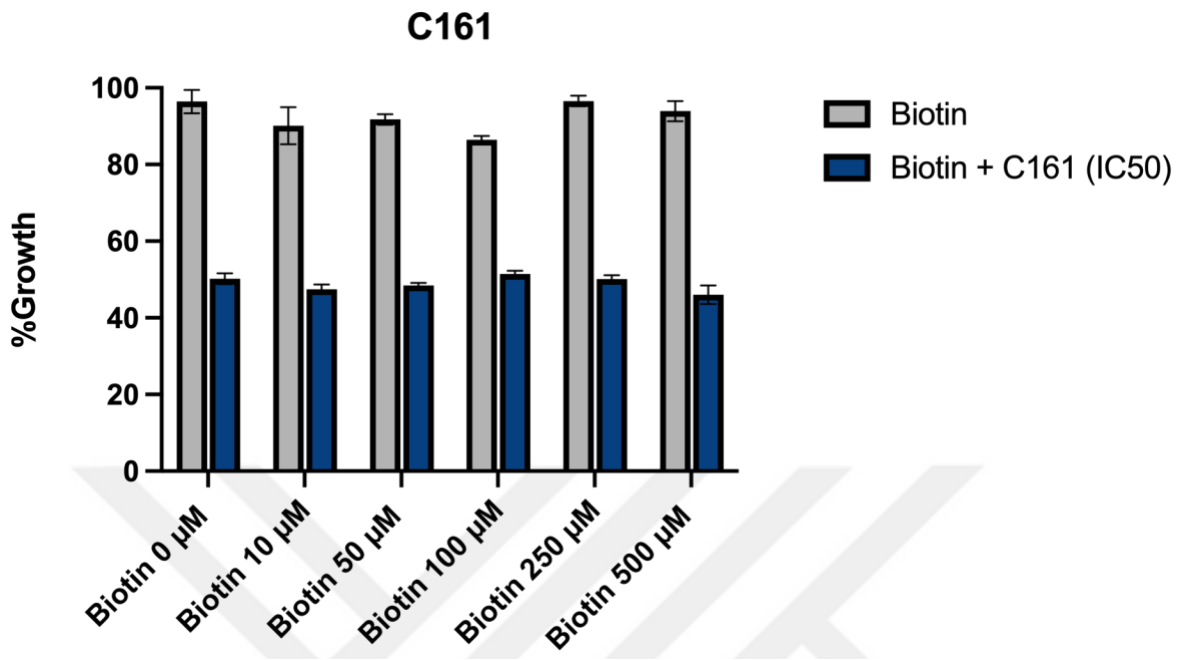

Figure 3. 8. Free biotin doesn't compete with biotinylated compounds in DU145 cells.

DU145 cells were pre-incubated with biotin and treatment with indicated compounds was performed afterwards. Treatment with compounds lasts 48 hours and biotin was renewed daily.

3.5. EB38 and Biotinylated Derivatives Halt 3D Growth of Spheroid Models

So far, we have characterized anti-growth capacity of EB38 and its biotinylated derivatives in 2D cellular models. We desired to translate our findings to 3D model, which is more physiologically relevant environment. In collaboration with Bilkent University, UNAM, Yeşilöz Research Group (Servin Bagheralmoosavi and Gürkan Yeşilöz), spheroids were generated with C4-2 cells and once they formed tight spheroids, they are treated with wide range of equimolar concentrations of compounds to examine effects of compounds on growth of spheroids. For high doses of compounds like 5 µM and 10 µM growth inhibition of spheroids appear to be in similar levels while the differences in growth inhibition capacity of EB38 and C160 are more obvious with lower concentrations. For EB38-treated spheroids, we detected preservation of integrity of spheroids until 3 µM while treatment with 1.5 µM of C160 and C161 is sufficient to lead to distortions in

spheroid integrity (Figure 3.9). When growth of spheroids is normalized to their "Day 0" counterparts, we detect that C160 is significantly induced better inhibition of spheroid growth compared to both EB38 and C161 (Figure 3.9). C161 treatment also halted growth of spheroid and disrupted spheroid integrity. However, C160 appeared to be the most efficient compound among them.

A)

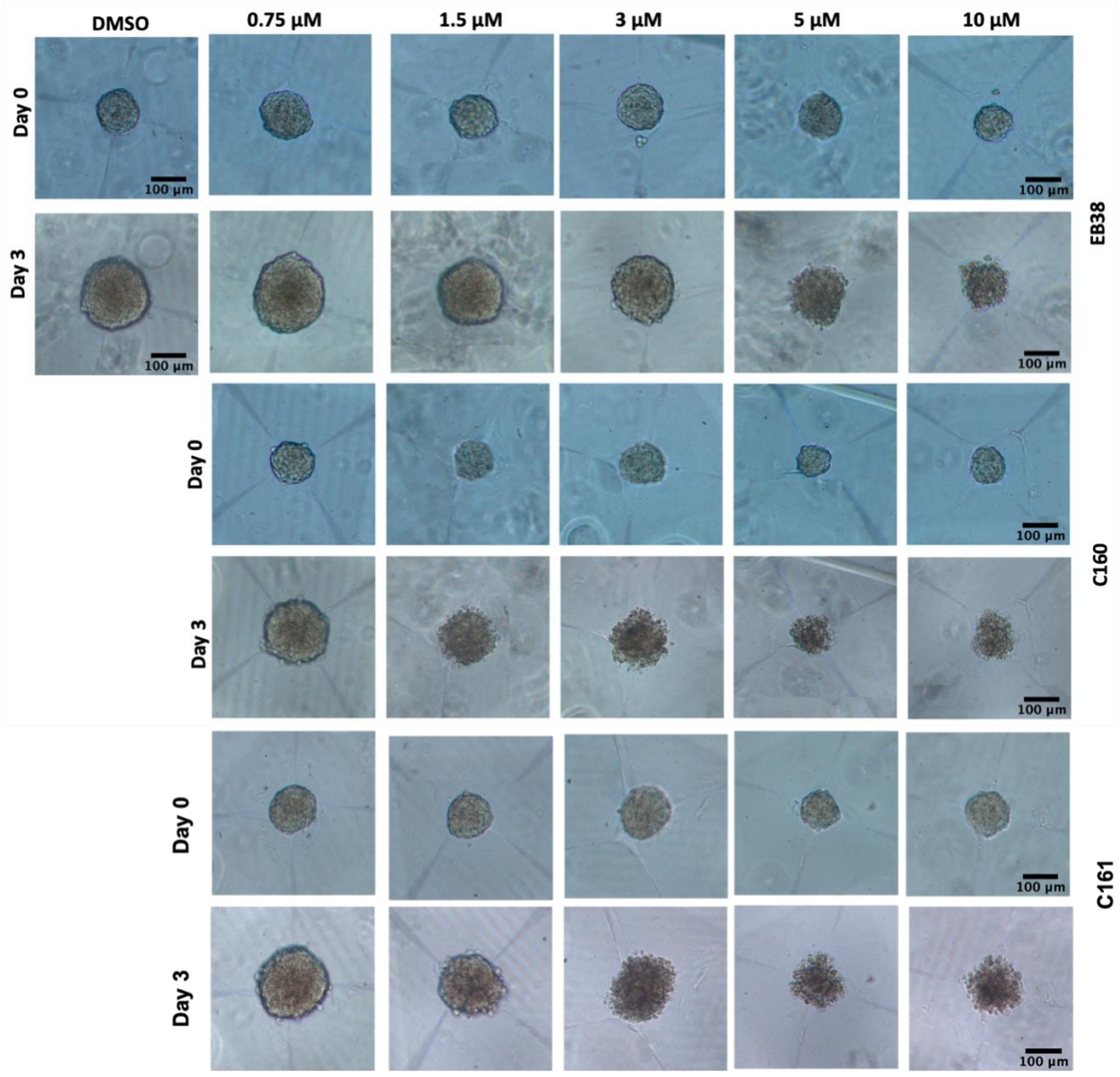

B)

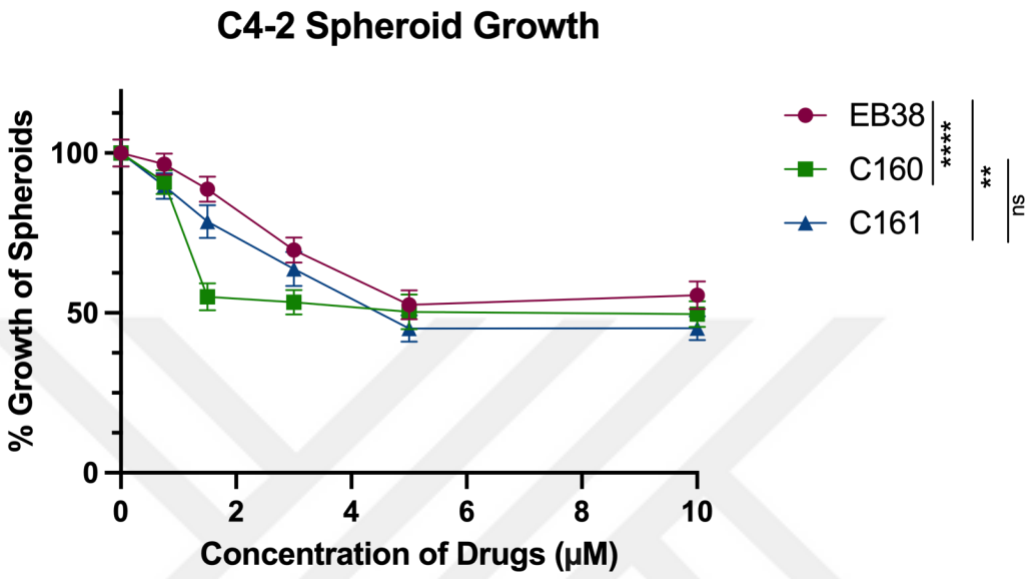

Figure 3. 9. Biotinylated compounds suppress growth of C4-2 spheroids in 3D models. Spheroid growth experiments were performed in collaboration with Bilkent University, UNAM, Yeşilöz Research Group (Servin Bagheralmoosavi and Gürkan Yeşilöz). Spheroids were treated with compounds for 3 days after forming tight spheroids. A) Representative images of C4-2 spheroids were given. B) Dose – response graphs showing growth of spheroids were drawn. Growth of spheroids was quantified based on spheroid sizes measured. Growth of spheroids was normalized with respect to day 0 measurements, followed by normalization with respect to DMSO group. Experiments were performed in triplicates, n > 20. Statistical analysis was performed by two-way ANOVA followed by Tukey's multiple comparisons test. Error bars represent SEM. * $p < 0.05$; ** $p < 0.01$; *** $p < 0.001$; **** $p < 0.0001$

3.6. Neither EB38 nor its Biotinylated Derivatives Cause Early-Developmental Stage Toxicity in Zebrafish

We wanted to investigate whether EB38 and its biotinylated derivatives result in any toxic effects, in order to evaluate safety of compounds and to determine whether growth inhibition observed in 2D and 3D assays and apoptosis are due to general toxicity of compounds. For this reason, we decided to test these compounds on zebrafish larvae because of their short generation time and rapid embryonic development (Teame et al., 2019). In collaboration with Konu Group (Rana Acar), zebrafish larvae were treated with from 2 dpf to 5 dpf with 2 µM, 5 µM, and 10 µM of each compound. Compounds were renewed daily. Time period between 2 dpf and 5 dpf correspond to early developmental stage of zebrafish where they are more susceptible to toxicity and any potential toxicity can be detected through observation of morphological abnormalities. At the end of the experiment, no morphological abnormalities were observed in zebrafish larvae (Figure 3.10). Standard length of zebrafish was measured to evaluate if they develop normally. Compound treatment didn't lead to any developmental delay. Zebrafish larvae reached their expected length and there was no difference compared to DMSO-treated group in terms of standard length.

A)

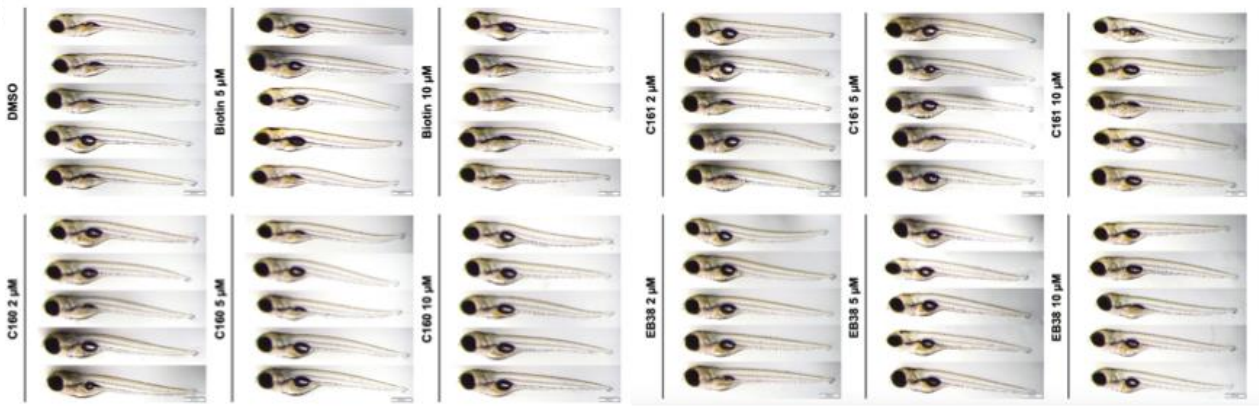

B)

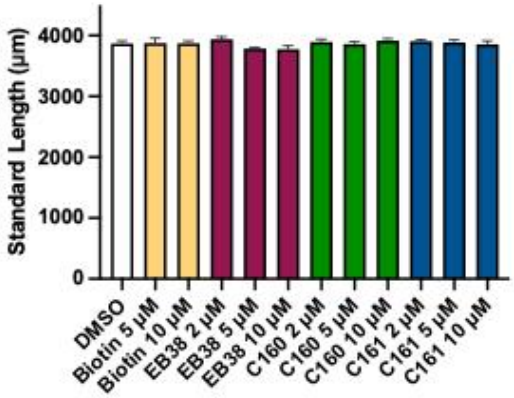

C)

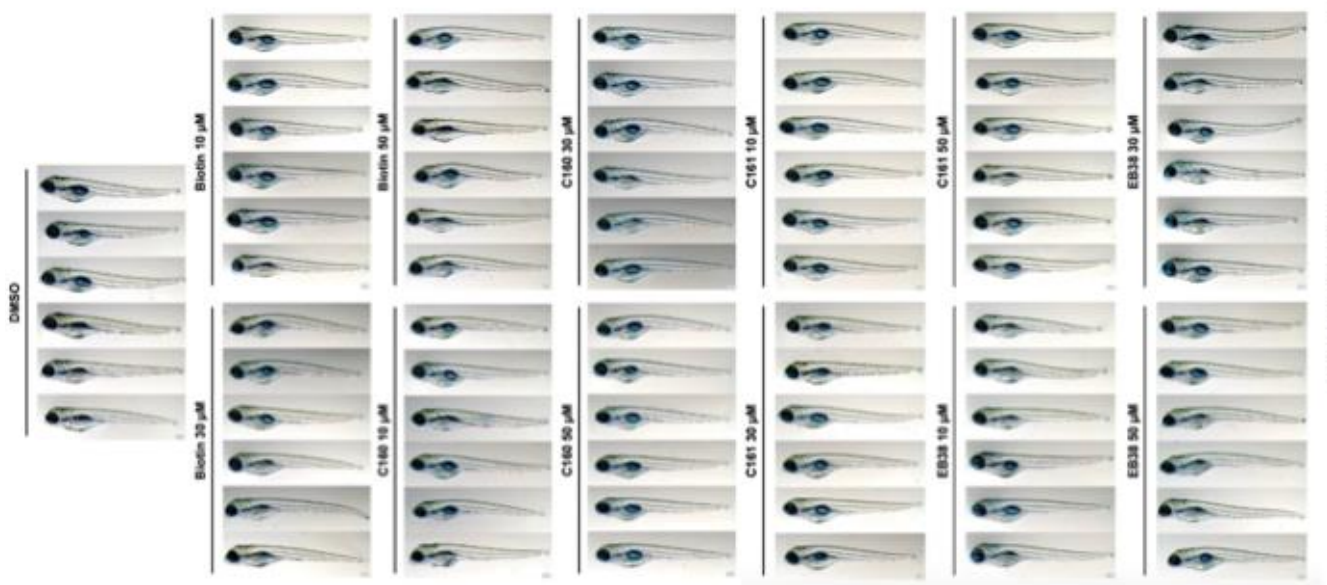

D)

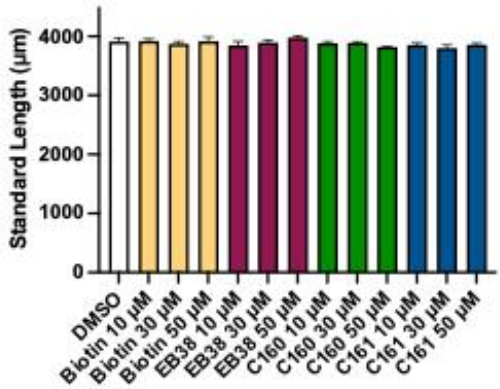

Figure 3. 10. Biotinylated compounds do not induce toxicity during early development of zebrafish larvae. Zebrafish toxicity experiments were performed in collaboration with Konu

Group. A) Zebrafish embryos were treated with lower doses of compounds from 2 dpf to 5 dpf. B) Standard length of zebrafish after treatment was measured. Error bars represent SEM, n = 18. C) Zebrafish embryos were treated with higher doses of compounds from 2 dpf to 5 dpf. Standard length of zebrafish after treatment was measured. Error bars represent SEM, n = 18. * $p < 0.05$, ** $p < 0.01$; *** $p < 0.001$; **** $p < 0.0001$

Zebrafish toxicity experiments were extended to include higher concentration of compounds. This time zebrafish larvae were treated with 10 μM, 30 μM, and 50 μM of each compound, which are considerably higher than doses used in growth inhibition experiments. EB38 and its biotinylated derivatives didn't induce toxicity even with higher doses. Morphological development of zebrafish larvae throughout the treatment period proceeded normally (Figure 3.10) and their standard length appeared to be almost the same with the DMSO-treated group. These findings suggest that EB38 and its derivatives have safe profile and growth inhibition we observed was not due to general toxicity.

4. DISCUSSION

In 2022, number of people died of cancer is 9.74 M and this number of deaths is expected to rise in the future years (The International Agency for Research on Cancer (IARC), n.d.), indicating that cancer will remain major health challenge. Although current therapies enable many patients to survive and recover, they remain inadequate to fully eradicate cancer because of issues such as resistance, toxic effects, and relapse (Davodabadi et al., 2023). This necessitates the development of novel anticancer therapy in order to reduce number of patients dying. In that regard, isoxazoles - subclass of heterocycles - appear to be promising pharmacophore that can be incorporated in anticancer agents.

We extended previous work where isoxazole based compound EB38 was characterized for its antitumorigenic potential (Turanlı et al., 2022). In that study, it was demonstrated that isoxazole based EB38 can inhibit growth of cancer cells in 2D model and suppress growth of breast and liver cancer xenografts. Additionally, EB38 was shown to initiate apoptotic-cell death in cancer cells. These findings laid the groundwork for our current study. Here, we further characterized antitumorigenic potential of EB38 and investigated biotin conjugated derivatives of EB38 to address the question of how biotin conjugation contributes to efficiency of anticancer compounds. In the literature, it is suggested that synthesizing biotinylated compounds can enhance intracellular accumulation of compounds within cancer cells, thereby increasing cytotoxicity. Consistent with these reports, our findings reveal that biotin conjugation enhances antitumorigenic potential of isoxazole based EB38.

Overexpression of vitamin transport mechanisms in cancer cells can be exploited to efficiently and selectively deliver drugs into cancer cells. Among these vitamins, conjugation with biotin (vitamin

B) appears as a promising strategy to enhance the delivery of drugs into cancer cells. Conjugating compounds with folate and B12 is also characterized in drug design as well. However, compared to folate and B12 receptors, biotin receptors are more overexpressed in cancer cells (Russell-Jones et al., 2004), contributing to specific delivery of biotin-conjugated compounds. Also, larger size of folate and vitamin B12 may interfere with drug activity, leading to more steric hinderance with these vitamins. In contrast, biotin is relatively small (Karalia & Meena, 2025). This makes biotin conjugation pharmacodynamically more favorable over other vitamins. Additionally, noncovalent interaction between biotin and streptavidin is among the strongest interactions (B. Liu et al., 2024). This enables to purify molecular targets of biotin conjugated compounds through streptavidin pull down studies. Similarly, molecular imaging of biotin conjugated compounds can be carried out using streptavidin conjugated Alexa Fluor. With this advantage, biotin conjugation provides dual utilities which allows to carry out enhanced drug delivery as well as detection.

Our proliferation assays conducted with a panel of cancer cells demonstrate that biotinylated C160 and C161 exert more enhanced cytotoxicity compared to EB38. This pattern was consistently observed in all cancer cell lines. In this panel, we included cancer cell lines with different molecular characteristics in order to investigate feasibility of compounds in different cancer types. We found that all prostate, breast, and liver cancers tested were more susceptible to growth inhibition by biotin conjugated derivatives, highlighting the potential use of biotinylation as a strategy to increase cytotoxicity.

Additionally, in proliferation assays, it is observed that at higher concentrations, all compounds induced comparable levels of growth inhibition. However, at lower concentrations, the differences

in the cytotoxic capacities of EB38 and C160-C161 became markedly apparent, differentiating their cytotoxic capacities. In drug design, it is desired to have maximum response to compound with minimized concentrations to reduce side effects. In that regard, biotinylation of compounds appears as advantageous strategy since it enables to reduce possible side effects with the allowance of use of lower doses.

We also translated our findings into 3D spheroid models, where growth inhibition capacity of compounds was characterized. We demonstrated that with the lower concentration of C160 we can halt growth of spheroids and disrupt integrity of spheroids, while higher concentrations of EB38 and C161 are required to obtain the same level of growth inhibition and disrupted integrity. Translating our findings in 3D spheroid model is important since they better mimic physiological environment of tumor compared to 2D models (Xie et al., 2023). Moreover, in 2D cell culture models, compounds are equally accessible to each cell while in 3D models we can better recapitulate tumor environment where accessibility to compounds is restricted.

Our 2D and 3D growth experiments revealed that biotinylated C160 exerts better antitumorigenic properties compared to PEG-biotinylated C161. PEGylation of compounds is a chemical strategy employed to improve water solubility of compounds, helping compounds remain in the aqueous environment surrounding cells and serve as flexible linker to prevent steric hinderance (Veronese & Mero, 2008). Despite its chemical utility, our cell proliferation assays and 3D spheroid experiments proposed that because of the increased size of C161 due to PEG linker addition, it might not be penetrating into cells efficiently, resulting in less efficient growth inhibition than C160 - but still more efficient compared to EB38. Especially with the spheroid experiments, where

size of compounds plays a critical role in drug penetration, growth inhibition induced by C161 may have been adversely affected due to reduced accessibility of compounds. Moreover, molecular docking analysis conducted using Autodock Vina revealed that C161 exhibited more variable binding affinities towards available crystal structures of JAK1 catalytic site while binding affinities of EB38 and C160 for JAK1 catalytic site are more robust. This observation may be explained by the addition of PEG into structure of C161. Greater size of C161 upon PEGylation might disrupt the favorable binding of C161 into certain crystal structures of JAK1 catalytic site. These propose that although PEGylation is utilized with the aim of enhancing drug efficiency, molecular size of compounds is also another parameter that needs to be optimized in drug design.

We also revealed that EB38 and its biotinylated derivatives lead to apoptotic cell death in cancer cells, as indicated by cleavage of caspase 3/7 and PARP. Notably, magnitude of cleavage of proapoptotic proteins was greater in C160- and C161 treated cell lines in comparison to EB38-treated lines. This emphasizes that biotin conjugation potentiates pro-apoptotic capacity of compounds.

To gain insights into working mechanism of compounds, we performed western blot experiments targeting JAK/STAT and PI3K pathway. JAK/STAT pathway is responsible for cellular growth, immunity, survival (La Fortezza et al., 2016; Hu et al., 2021). Similarly, PI3K pathway also regulates proliferation, survival, etc. and frequently dysregulated in cancers. (Rodgers et al., 2017). Therefore, they have potential to be possible targets of compounds. Our biochemical characterizations revealed JAK/STAT is the primary target of our compounds while PIP3 biosensor assay showed that PI3K is unlikely to be directly targeted by the compounds. Moreover,

biotinylated C160 and C161 more potently suppress p-STAT1 and p-JAK1, whose phosphorylations are associated with activated JAK/STAT pathway. To confirm our findings, we conducted computational docking analysis where binding affinities of EB38 and its derivatives were investigated with respect to FDA-approved JAK1 inhibitor, Ruxolitinib. EB38 and C160 were emerged as compounds efficiently docked to catalytic site of JAK1 enzyme. All in all, these results imply that JAK/STAT pathway can be the primary target for mediating the activity of these compounds while PI3K pathway may be modulated secondarily by EB38 and its biotinylated derivatives.

Since our ultimate aim is to potentially use these compounds as anticancer drugs, evaluating their safety profiles is also of critical importance. First, we started with assessing cytotoxicity of compounds in non-tumorigenic cells lines (MCF10A, hTERT-RPE1, and MEF). Viability of C160- and C161- treated healthy lines were reduced significantly compared to EB38-treated cells, but this reduction is less apparent compared to cancer cells. We observed that compounds are also able inhibit proliferation of healthy cells despite being to a lesser extent. Cell lines used as non-tumorigenic lines may not be true representation of normal cells because they underwent immortalization process and have high proliferation capacity. We propose that compounds are likely to inhibit growth of highly proliferative cells. That could be the reason for observing inhibition with healthy cells. Building on these findings, testing safety of compounds in in vivo settings would be more relevant like zebrafish larvae. We performed treatment with compounds while zebrafish were in their early developmental stages where they are more fragile and sensitive towards toxic agents (Cassar et al., 2019). In zebrafish toxicity tests, survival, developmental abnormalities, cardiac function, motor abilities, organ development etc. are taken into

consideration while evaluating toxicity of compounds. Especially heart-rate can be tracked in zebrafish embryo toxicity assays since toxicants can disrupt heartbeat. Also, pericardial edema can be observed in embryos as general response when exposed to toxic agents. Additionally, yolk sac is a critical structure that is assessed to understand toxicity of compounds. Yolk sac edema is pathology observed when nutrient absorption by embryos were reduced (Chahardehi et al., 2020). With respect to these parameters considered in zebrafish toxicity tests, our compounds appeared to induce no toxicity - even at the highest treatment concentration, which exceeds concentrations used in proliferation assay - as we interpreted from proper development of larvae allowing to reach expected body length, lack of yolk sac edema, and no presence of morphological abnormalities. (Detailed description on yolk sac edema and growth retardation observed under toxic conditions in zebrafish embryos can be found in Rana Acar's thesis). Although we observed growth inhibition with non-tumorigenic cell lines, absence of toxicity in zebrafish larvae provides promising evidence regarding safety of the use of compounds.

Although there several reports published providing evidences for enhanced uptake of biotin-conjugated compounds, understanding of which mechanisms facilitate accumulation of biotin-conjugated compounds in the cells remain unclear. To this end, we conducted free-biotin competition assay with DU145 cells. The reason why we included this cell line is that differences between IC50 of non-biotinylated compound and biotinylated compounds are the most apparent. We observed that in the presence of increasing dosages of free biotin, EB38 and biotinylated C160 and C161 continue to exert their cytotoxic activities. If there were a competition between free biotin and biotinylated compounds, we would observe decreased cytotoxicity of C160 and C161 while EB38's cytotoxicity would not been affected by free biotin. Lack of competition with biotin

suggest us that biotinylated C160 and C161 are not taken up by SMVT transporters, which are known to be saturable with free biotin. In line with the previous studies in the literature, we propose that in the tested cell line, alternative, non-competitive routes such as endocytosis may regulate biotin uptake (Tripathi et al., 2023).

5. CONCLUSION AND FUTURE PERSPECTIVES

In this project we investigated and demonstrated antitumorigenic potential of EB38 and its biotinylated derivatives from multiple perspectives – including antiproliferative effects, proapoptotic activity, and JAK1 inhibitory activity- and proposed biotinylation of compounds as a strategy to enhance their activity. So far, we have translated our findings into 3D spheroid models. However, in future studies it is needed to go beyond in vitro studies and recapitulate our findings in in vivo mouse models to understand how these compounds behave in complex physiological environment, to evaluate toxicity of compounds, and to establish pharmacokinetic and pharmacodynamic profiles of the compounds.

Another important point of future studies will be investigating the mechanisms that contribute to efficient uptake of biotinylated compounds. Our free biotin competition experiments suggest that their uptake is unlikely to be mediated by SMVTs. However, further work is required to make our hypothesis solid. We plan to perform competition experiments with other cell lines to identify biotin uptake mechanisms.

6. REFERENCES

Arya, G. C., Kaur, K., & Jaitak, V. (2021). Isoxazole derivatives as anticancer agent: A review on synthetic strategies, mechanism of action and SAR studies. *European Journal of Medicinal Chemistry*, *221*, 113511. https://doi.org/10.1016/j.ejmech.2021.113511

Cassar, S., Adatto, I., Freeman, J. L., Gamse, J. T., Iturria, I., Lawrence, C., Muriana, A., Peterson, R. T., Van Cruchten, S., & Zon, L. I. (2019). Use of zebrafish in drug discovery toxicology. *Chemical Research in Toxicology*, *33*(1), 95–118. https://doi.org/10.1021/acs.chemrestox.9b00335

Chahardehi, A. M., Arsad, H., & Lim, V. (2020). Zebrafish as a successful animal model for screening toxicity of medicinal plants. *Plants*, *9*(10), 1345. https://doi.org/10.3390/plants9101345

Daberkow, R. L., White, B. R., Cederberg, R. A., Griffin, J. B., & Zempleni, J. (2003). Monocarboxylate transporter 1 mediates biotin uptake in human peripheral blood mononuclear cells. *Journal of Nutrition*, *133*(9), 2703–2706. https://doi.org/10.1093/jn/133.9.2703

Davodabadi, F., Sajjadi, S. F., Sarhadi, M., Mirghasemi, S., Hezaveh, M. N., Khosravi, S., Andani, M. K., Cordani, M., Basiri, M., & Ghavami, S. (2023). Cancer chemotherapy resistance: Mechanisms and recent breakthrough in targeted drug delivery. *European Journal of Pharmacology*, *958*, 176013. https://doi.org/10.1016/j.ejphar.2023.176013

Fraser, M., Zhao, H., Luoto, K. R., Lundin, C., Coackley, C., Chan, N., Joshua, A. M., Bismar, T. A., Evans, A., Helleday, T., & Bristow, R. G. (2011). PTEN Deletion in Prostate Cancer Cells Does Not Associate with Loss of RAD51 Function: Implications for Radiotherapy and Chemotherapy. *Clinical Cancer Research*, *18*(4), 1015–1027. https://doi.org/10.1158/1078-0432.ccr-11-2189

Gan, L., Chen, S., Wang, Y., Watahiki, A., Bohrer, L., Sun, Z., Wang, Y., & Huang, H. (2009). Inhibition of the androgen receptor as a novel mechanism of taxol chemotherapy in

prostate cancer. *Cancer Research*, *69*(21), 8386–8394. https://doi.org/10.1158/0008-5472.can-09-1504

Gunawardane, R. N., Nepomuceno, R. R., Rooks, A. M., Hunt, J. P., Ricono, J. M., Belli, B., & Armstrong, R. C. (2013). Transient Exposure to Quizartinib Mediates Sustained Inhibition of FLT3 Signaling while Specifically Inducing Apoptosis in FLT3-Activated Leukemia Cells. *Molecular Cancer Therapeutics*, *12*(4), 438–447. https://doi.org/10.1158/1535-7163.mct-12-0305

Hu, X., Li, J., Fu, M., Zhao, X., & Wang, W. (2021). The JAK/STAT signaling pathway: from bench to clinic. *Signal Transduction and Targeted Therapy*, *6*(1). https://doi.org/10.1038/s41392-021-00791-1

Huang, Z., Yu, P., & Tang, J. (2020). Characterization of Triple-Negative Breast Cancer MDA-MB-231 Cell Spheroid Model *OncoTargets and Therapy*, *Volume 13*, 5395–5405. https://doi.org/10.2147/ott.s249756

Hui, L., Zheng, Y., Yan, Y., Bargonetti, J., & Foster, D. A. (2006). Mutant p53 in MDA-MB-231 breast cancer cells is stabilized by elevated phospholipase D activity and contributes to survival signals generated by phospholipase D. *Oncogene*, *25*(55), 7305–7310. https://doi.org/10.1038/sj.onc.1209735

Jung, D., Maiti, S., Lee, J. H., Lee, J. H., & Kim, J. S. (2014). Rational design of biotin–disulfide–coumarin conjugates: a cancer targeted thiol probe and bioimaging. *Chemical Communications*, *50*(23), 3044. https://doi.org/10.1039/c3cc49790a

Karalia, S., & Meena, V. K. (2025). Biotin: DNA to Diet. *The Journal of Nutritional Biochemistry*, 110081. https://doi.org/10.1016/j.jnutbio.2025.110081

Kang, M., Lee, H., Lee, J., Ku, J., Lee, K. P., Kelley, M. J., Won, Y., Kim, S., & Park, J. (1996). Mutation ofp53 gene in hepatocellular carcinoma cell lines with HBX DNA. *International Journal of Cancer*, *67*(6), 898–902. https://doi.org/10.1002/(sici)1097-0215(19960917)67:6

Keskin, F., Suhre, A., Kose, K., Ersahin, T., Cetin, A. E., & Cetin-Atalay, R. (2013). Image classification of human carcinoma cells using complex Wavelet-Based covariance descriptors. *PLoS ONE*, *8*(1), e52807. https://doi.org/10.1371/journal.pone.0052807

Kuroishi, T., Rios-Avila, L., Pestinger, V., Wijeratne, S. S., & Zempleni, J. (2011). Biotinylation is a natural, albeit rare, modification of human histones. *Molecular Genetics and Metabolism*, *104*(4), 537–545. https://doi.org/10.1016/j.ymgme.2011.08.030

La Fortezza, M., Schenk, M., Cosolo, A., Kolybaba, A., Grass, I., & Classen, A. (2016). JAK/STAT signalling mediates cell survival in response to tissue stress. *Development*, *143*(16), 2907–2919. https://doi.org/10.1242/dev.132340

Lee, K., Lee, J., Han, S., Im, S., Kim, T., Oh, D., & Bang, Y. (2011). Antitumor activity of NVP-AUY922, a novel heat shock protein 90 inhibitor, in human gastric cancer cells is mediated through proteasomal degradation of client proteins. *Cancer Science*, *102*(7), 1388–1395. https://doi.org/10.1111/j.1349-7006.2011.01944.x

León-Del-Río, A. (2019). Biotin in metabolism, gene expression, and human disease. *Journal of Inherited Metabolic Disease*, *42*(4), 647–654. https://doi.org/10.1002/jimd.12073

Li, J. J. (2013). *Heterocyclic chemistry in drug discovery*. http://ci.nii.ac.jp/ncid/BB13953817

Liu, B., Zhou, H., Tan, L., Siu, K. T. H., & Guan, X. (2024). Exploring treatment options in cancer: Tumor treatment strategies. *Signal Transduction and Targeted Therapy*, *9*(1). https://doi.org/10.1038/s41392-024-01856-7

Liu, W., Samanta, S. K., Smith, B. D., & Isaacs, L. (2017). Synthetic mimics of biotin/(strept)avidin. *Chemical Society Reviews*, *46*(9), 2391–2403. https://doi.org/10.1039/c7cs00011a

Lv, L., Liu, C., Chen, C., Yu, X., Chen, G., Shi, Y., Qin, F., Ou, J., Qiu, K., & Li, G. (2016). Quercetin and doxorubicin co-encapsulated biotin receptor-targeting nanoparticles for minimizing drug resistance in breast cancer. *Oncotarget*, *7*(22), 32184–32199. https://doi.org/10.18632/oncotarget.8607

Maiti, S., Park, N., Han, J. H., Jeon, H. M., Lee, J. H., Bhuniya, S., Kang, C., & Kim, J. S. (2013). Gemcitabine–Coumarin–Biotin conjugates: a target specific theranostic anticancer prodrug. *Journal of the American Chemical Society*, *135*(11), 4567–4572. https://doi.org/10.1021/ja401350x

Malik, U., & Pal, D. (2024). Isoxazole compounds: unveiling the synthetic strategy, In-silico SAR & Toxicity studies and future perspective as PARP inhibitor in cancer therapy. *European Journal of Medicinal Chemistry*, *279*, 116898. https://doi.org/10.1016/j.ejmech.2024.116898

McMahon, R. J. (2002). BIOTIN IN METABOLISM AND MOLECULAR BIOLOGY. *Annual Review of Nutrition*, *22*(1), 221–239. https://doi.org/10.1146/annurev.nutr.22.121101.112819

Montenegro, R. C., Clark, P. G., Howarth, A., Wan, X., Ceroni, A., Siejka, P., Nunez-Alonso, G. A., Monteiro, O., Rogers, C., Gamble, V., Burbano, R., Brennan, P. E., Tallant, C., Ebner, D., Fedorov, O., O'Neill, E., Knapp, S., Dixon, D., & Müller, S. (2016). BET inhibition as a new strategy for the treatment of gastric cancer. *Oncotarget*, *7*(28), 43997–44012. https://doi.org/10.18632/oncotarget.9766

Morita, T., Yugandar, S., Fuse, S., & Nakamura, H. (2018). Recent progresses in the synthesis of functionalized isoxazoles. *Tetrahedron Letters*, *59*(13), 1159–1171. https://doi.org/10.1016/j.tetlet.2018.02.020

Ostojic, A., Vrhovac, R., & Verstovsek, S. (2011). Ruxolitinib: a new JAK1/2 inhibitor that offers promising options for treatment of myelofibrosis. *Future Oncology*, *7*(9), 1035–1043. https://doi.org/10.2217/fon.11.81

Pandeya, A., Yang, L., Alegun, O., Karunasena, C., Risko, C., Li, Z., & Wei, Y. (2021). Biotinylation as a tool to enhance the uptake of small molecules in Gram-negative bacteria. *PLoS ONE*, *16*(11), e0260023. https://doi.org/10.1371/journal.pone.0260023

Patil, B. M., Shinde, S. K., Jagdale, A. A., Jadhav, S. D., & Patil, S. S. (2021). Fruit Extract of Averrhoa bilimbi: A Green Neoteric Micellar Medium for Isoxazole and Biginelli-Like

Synthesis. *Research on Chemical Intermediates*, *47*(10), 4369–4398. https://doi.org/10.1007/s11164-021-04539-y

Peřina, M., Kiss, M. A., Bělíček, J., Vojáčková, V., Veselá, D., Minorics, R., Zupko, I., Frank, É., & Jorda, R. (2025). Isoxazole-Based compounds targeting the Taxane-Binding site of Tubulin. *Archiv Der Pharmazie*, *358*(7). https://doi.org/10.1002/ardp.70031

Polyak, S. W. (2015). Mechanisms of biotin transport. *Biochemistry & Analytical Biochemistry*, *04*(04). https://doi.org/10.4172/2161-1009.1000210

Puisieux, A., Galvin, K., Troalen, F., Bressac, B., Marcais, C., Galun, E., Ponchel, F., Yakicier, C., Ji, J., & Ozturk, M. (1993). Retinoblastoma and p 53 tumor suppressor genes in human hepatoma cell lines. *The FASEB Journal*, *7*(14), 1407–1413. https://doi.org/10.1096/fasebj.7.14.8224613

Ren, W. X., Han, J., Uhm, S., Jang, Y. J., Kang, C., Kim, J., & Kim, J. S. (2015). Recent development of biotin conjugation in biological imaging, sensing, and target delivery. *Chemical Communications*, *51*(52), 10403–10418. https://doi.org/10.1039/c5cc03075g

Rodgers, S. J., Ferguson, D. T., Mitchell, C. A., & Ooms, L. M. (2017). Regulation of PI3K effector signalling in cancer by the phosphoinositide phosphatases. *Bioscience Reports*, *37*(1). https://doi.org/10.1042/bsr20160432

Rodriguez-Melendez, R., & Zempleni, J. (2003). Regulation of gene expression by biotin☆ (review). *The Journal of Nutritional Biochemistry*, *14*(12), 680–690. https://doi.org/10.1016/j.jnutbio.2003.07.001

Russell-Jones, G., McTavish, K., McEwan, J., Rice, J., & Nowotnik, D. (2004). Vitamin-mediated targeting as a potential mechanism to increase drug uptake by tumours. *Journal of Inorganic Biochemistry*, *98*(10), 1625–1633. https://doi.org/10.1016/j.jinorgbio.2004.07.009

Said, H. M. (1999). Cellular uptake of biotin: mechanisms and regulation. *Journal of Nutrition*, *129*(2), 490S-493S. https://doi.org/10.1093/jn/129.2.490s

Said, H. M. (2008). Cell and molecular aspects of human intestinal biotin absorption. *Journal of Nutrition*, *139*(1), 158–162. https://doi.org/10.3945/jn.108.092023

Said, H. M. (2011). Biotin: biochemical, physiological and clinical aspects. *Sub-cellular Biochemistry/Subcellular Biochemistry*, 1–19. https://doi.org/10.1007/978-94-007-2199-9_1

Shaik, A., Bhandare, R. R., Palleapati, K., Nissankararao, S., Kancharlapalli, V., & Shaik, S. (2020). Antimicrobial, antioxidant, and anticancer activities of some novel isoxazole ring containing chalcone and dihydropyrazole derivatives. *Molecules*, *25*(5), 1047. https://doi.org/10.3390/molecules25051047

Singh, M., Afonso, J., Sharma, D., Gupta, R., Kumar, V., Rani, R., Baltazar, F., & Kumar, V. (2023). Targeting monocarboxylate transporters (MCTs) in cancer: How close are we to the clinics? *Seminars in Cancer Biology*, *90*, 1–14. https://doi.org/10.1016/j.semcancer.2023.01.007

Sochacka-Ćwikła, A., Mączyński, M., & Regiec, A. (2022). FDA-Approved Small Molecule Compounds as Drugs for Solid Cancers from Early 2011 to the End of 2021. *Molecules*, *27*(7), 2259. https://doi.org/10.3390/molecules27072259

Stanger, O. (2011). Water soluble vitamins. In *Sub-cellular biochemistry/Subcellular biochemistry*. https://doi.org/10.1007/978-94-007-2199-9

Subedi, D., Ashley, A. K., Chavez, M. V., & Smirnov, S. N. (2020). Mixed silane monolayers reveal the disparity of biotin and folate in targeting cancer cells. *ACS Applied Nano Materials*, *3*(6), 5372–5380. https://doi.org/10.1021/acsanm.0c00731

Tandon, R., Singh, I., Luxami, V., Tandon, N., & Paul, K. (2018). Recent Advances and Developments of in vitro Evaluation of Heterocyclic Moieties on Cancer Cell Lines. *The Chemical Record*, *19*(2–3), 362–393. https://doi.org/10.1002/tcr.201800024

Teame, T., Zhang, Z., Ran, C., Zhang, H., Yang, Y., Ding, Q., Xie, M., Gao, C., Ye, Y., Duan, M., & Zhou, Z. (2019). The use of zebrafish (Danio rerio) as biomedical models. *Animal Frontiers*, *9*(3), 68–77. https://doi.org/10.1093/af/vfz020

The International Agency for Research on Cancer (IARC). (n.d.). *Global Cancer Observatory*. https://gco.iarc.fr/en

Tong, L. (2012). Structure and function of biotin-dependent carboxylases. *Cellular and Molecular Life Sciences*, *70*(5), 863–891. https://doi.org/10.1007/s00018-012-1096-0

Tripathi, R., Guglani, A., Ghorpade, R., & Wang, B. (2023). Biotin conjugates in targeted drug delivery: is it mediated by a biotin transporter, a yet to be identified receptor, or (an)other unknown mechanism(s)? *Journal of Enzyme Inhibition and Medicinal Chemistry*, *38*(1). https://doi.org/10.1080/14756366.2023.2276663

Turanlı, S., Nalbat, E., Lengerli, D., İbiş, K., Ergün, S. G., Güzelcan, E. A., Muyan, M., Cetin-Atalay, R., Çalışkan, B., & Banoglu, E. (2022). Vicinal Diaryl-Substituted Isoxazole and Pyrazole Derivatives with In Vitro Growth Inhibitory and In Vivo Antitumor Activity. *ACS Omega*, *7*(41), 36206–36226. https://doi.org/10.1021/acsomega.2c03405

Vadlapudi, A. D., Vadlapatla, R. K., & Mitra, A. K. (2012). Sodium Dependent Multivitamin Transporter (SMVT): a potential target for drug delivery. *Current Drug Targets*, *13*(7), 994–1003. https://doi.org/10.2174/138945012800675650

Várnai, P., Rother, K. I., & Balla, T. (1999). Phosphatidylinositol 3-Kinase-dependent membrane association of the Bruton's tyrosine kinase pleckstrin homology domain visualized in single living cells. *Journal of Biological Chemistry*, *274*(16), 10983–10989. https://doi.org/10.1074/jbc.274.16.10983

Vashisht, K., Sethi, P., Bansal, A., & Bansal, P. (2024). Antimicrobial activity of isoxazole derivatives: A brief overview. *Vietnam Journal of Chemistry*. https://doi.org/10.1002/vjch.202400029

Veronese, F. M., & Mero, A. (2008). The impact of PEGylation on biological therapies. *BioDrugs*, *22*(5), 315–329. https://doi.org/10.2165/00063030-200822050-00004

Wang, C., Xiu, Y., Zhang, Y., Wang, Y., Xu, J., Yu, W., & Xing, D. (2024). Recent advances in Biotin-based therapeutic agents for cancer therapy. *Nanoscale*, *17*(4), 1812–1873. https://doi.org/10.1039/d4nr03729d

Wang, H., Zhou, Y., Chu, C., Xiao, J., Zheng, S., Korpal, M., Korn, J. M., Penaloza, T., Drake, R. R., Gan, W., & Gao, X. (2023). Generating a murine PTEN null cell line to discover the key role of P110B-PAK1 in Castration-Resistant prostate cancer invasion. *Molecular Cancer Research*, *21*(12), 1317–1328. https://doi.org/10.1158/1541-7786.mcr-22-0808

Wu, R., Ding, W., Liu, T., Zhu, H., Hu, Y., Yang, B., & He, Q. (2009). XN05, a novel synthesized microtubule inhibitor, exhibits potent activity against human carcinoma cells in vitro. *Cancer Letters*, *285*(1), 13–22. https://doi.org/10.1016/j.canlet.2009.04.042

Xie, R., Pal, V., Yu, Y., Lu, X., Gao, M., Liang, S., Huang, M., Peng, W., & Ozbolat, I. T. (2023). A comprehensive review on 3D tissue models: Biofabrication technologies and preclinical applications. *Biomaterials*, *304*, 122408. https://doi.org/10.1016/j.biomaterials.2023.122408

Yu, S., Kim, T., Yoo, K. H., & Kang, K. (2017). The T47D cell line is an ideal experimental model to elucidate the progesterone-specific effects of a luminal A subtype of breast cancer. *Biochemical and Biophysical Research Communications*, *486*(3), 752–758. https://doi.org/10.1016/j.bbrc.2017.03.114

7. APPENDIX

7.1. Copyright Permissions

Permission for the figure 1.1:

SPRINGER NATURE LICENSE
TERMS AND CONDITIONS

Aug 09, 2025

This Agreement between Melike Ergüven ("You") and Springer Nature ("Springer Nature") consists of your license details and the terms and conditions provided by Springer Nature and Copyright Clearance Center.

License Number	6084170518937
License date	Aug 08, 2025
Licensed Content Publisher	Springer Nature
Licensed Content Publication	Research on Chemical Intermediates
Licensed Content Title	Fruit Extract of Averrhoa bilimbi: A Green Neoteric Micellar Medium for Isoxazole and Biginelli-Like Synthesis
Licensed Content Author	Bhagyashree M. Patil et al
Licensed Content Date	Sep 8, 2021
Type of Use	Thesis/Dissertation
Requestor type	academic/university or research institute
Format	print and electronic
Portion	figures/tables/illustrations

Number of figures/tables/illustrations	1
Will you be translating?	no
Circulation/distribution	1 - 29
Author of this Springer Nature content	no
Title of new work	INVESTIGATION OF ANTITUMOR EFFECTS OF NOVEL ISOXAZOLE DERIVATIVES AND THE ROLE OF BIOTIN CONJUGATION IN THEIR EFFICACY
Institution name	Bilkent University
Expected presentation date	Aug 2025
Portions	Figure 1
The Requesting Person / Organization to Appear on the License	Melike Ergüven
Requestor Location	Melike Ergüven Eskibağlar Cad. No:56/22 Bağlıca ANKARA Ankara, 06790 Turkey
Order reference number	255
Billing Type	Invoice
	Melike Ergüven Eskibağlar Cad. No:56/22 Bağlıca ANKARA

Permission for the figure 1.2:

JOHN WILEY AND SONS LICENSE
TERMS AND CONDITIONS

Aug 09, 2025

This Agreement between Melike Ergüven ("You") and John Wiley and Sons ("John Wiley and Sons") consists of your license details and the terms and conditions provided by John Wiley and Sons and Copyright Clearance Center.

License Number	6084680642617
License date	Aug 09, 2025
Licensed Content Publisher	John Wiley and Sons
Licensed Content Publication	JOURNAL OF INHERITED METABOLIC DISEASE
Licensed Content Title	Biotin in metabolism, gene expression, and human disease
Licensed Content Author	Alfonso León-Del-Río
Licensed Content Date	Mar 19, 2019
Licensed Content Volume	42
Licensed Content Issue	4
Licensed Content Pages	8

Type of use	Dissertation/Thesis
Requestor type	University/Academic
Format	Print and electronic
Portion	Figure/table
Number of figures/tables	1
Will you be translating?	No
Title of new work	INVESTIGATION OF ANTITUMOR EFFECTS OF NOVEL ISOXAZOLE DERIVATIVES AND THE ROLE OF BIOTIN CONJUGATION IN THEIR EFFICACY
Institution name	Bilkent University
Expected presentation date	Aug 2025
Portions	Figure 1
The Requesting Person / Organization to Appear on the License	Melike Ergüven
Requestor Location	Melike Ergüven Eskibağlar Cad. No:56/22 Bağlıca ANKARA Ankara, 06790 Turkey
Order reference number	255